Journal of Great Lakes Research 42 (2016) 972–984

Contents lists available at ScienceDirect

Journal of Great Lakes Research

journal homepage: www.elsevier.com/locate/jglr

Evaluating the relationships between watershed physiography, land use patterns, and phosphorus loading in the bay of Quinte basin, Ontario, Canada

Dong-Kyun Kim [a], Samarth Kaluskar [a], Shan Mugalingam [b], George B. Arhonditsis [a,*]

[a] Ecological Modelling Laboratory, Department of Physical & Environmental Sciences, University of Toronto, Toronto, Ontario M1C1A4, Canada
[b] Lower Trent Conservation Authority, Trenton, Ontario K8V 5P4, Canada

ARTICLE INFO

Article history:
Received 21 February 2016
Accepted 26 June 2016
Available online 12 September 2016

Communicated by Craig Stow

Index words:
Bay of Quinte
Pattern recognition
Self-organizing map
TP loading
Watershed physiography

ABSTRACT

The Bay of Quinte, a Z-shaped embayment at the northeastern end of Lake Ontario, represents a characteristic case of an area of concern (AOC) where scientific uncertainty underlies management efforts to address eutrophication problems. The present study attempts to examine the relationships between total phosphorus (TP) (i.e., concentrations from point and non-point sources, net export, and yield) and watershed attributes, including land use cover and physiographic characteristics. Dynamic linear modeling is applied to assess temporal trends in the flow rates in five major tributaries of the area. Urbanized catchments near the Bay of Quinte show more dynamic flow patterns with significant within- and among-year variability and stronger response to local precipitation patterns. The "flashy" behavior of urban land is characterized by relatively high net TP export and TP yield. Self-organizing map analysis, classified the watershed into six distinct spatial clusters, representing two agricultural, one forested, one urban, one pasture-dominated, and one transitional area. Our study shows that agricultural and urban sites profoundly shape riverine TP dynamics. We also provide evidence that tributaries draining agricultural areas exhibit considerable variability, depending on management practices and soil properties. Excessive fertilizer or manure application in croplands, management practices (e.g., crop types and tillage methods) and soil hydrological characteristics (e.g., hydraulic conductivity and permeability) generally determine soil phosphorus level and consequent losses through erosion and runoff from agricultural sites. In a similar manner, pasture-based grazing systems appear to play an important role in modulating the fate and transport of phosphorus in the Bay of Quinte watershed.

Introduction

Despite decades of active research in the field of watershed science, there are still considerable gaps in our understanding of the complex interplay among hydrological factors, morphological/ geological features, land uses, and spatial patterns of the urban environment and agricultural activities that modulate the attenuation rates of nutrients and contaminants in a watershed context (Rode et al., 2010). Most watersheds of management interest in the Great Lakes area are not well studied, and therefore, one of the imperatives of the contemporary management practices is the development of methodological frameworks that can offer insights into the long-term watershed dynamics of urban and agricultural landscapes (Arhonditsis et al., 2016). The Bay of Quinte, a Z-shaped embayment at the northern end of Lake Ontario, has experienced a long history of ecological problems, such as toxic algal blooms, bacterial contamination, dominance (or invasion) of undesirable fish species, and destruction of wildlife habitats (Arhonditsis et al., 2016; Shimoda et al., 2016). To ameliorate these degradation issues, the Great Lakes Water Quality Agreement between the United States and Canada established a number of initiatives, objectives, and guidelines to restore and maintain physicochemical and biological integrity (USEPA, 1978). In particular, the Canadian government made a commitment to restore the bay by introducing a comprehensive action plan that primarily aimed to control nutrient loading from municipal sewage treatment plants (STPs) (BQRAP, 1987). These remedial measures have resulted in a dramatic reduction (>95%) of the phosphorus discharges from the 1960s, 215 kg d^{-1}, to the 2000s, <10 kg d^{-1} (Kinstler and Morley, 2011). Nonetheless, despite the substantial improvement of the ambient water quality conditions, high TP concentrations and harmful algal blooms remain a central issue in the system (Minns et al., 1986a). The Bay of Quinte is still one of the International Joint Commission's (IJC) 43 degraded sites or AOCs, as it experiences 11 out of 14 of the IJC's Beneficial Use Impairments (BUIs). Furthermore, zebra and quagga mussels (*Dreissena polymorpha* and *Dreissena bugensis*)

* Corresponding author. Tel.: +1 416 208 4858.
E-mail address: georgea@utsc.utoronto.ca (G.B. Arhonditsis).

http://dx.doi.org/10.1016/j.jglr.2016.07.008
0380-1330/

have invaded the bay since the mid-1990s, further complicating ecosystem structure and functioning (Dermott et al., 2003; Dermott and Bonnell, 2011).

Phosphorus export from the adjacent catchments and internal nutrient regeneration are both contributing to the eutrophication problems in the Bay of Quinte. The latter problem is associated not only with the sediment diagenesis processes but also the invasion of dreissenids that could potentially accelerate the internal loading rates of the system (Bailey et al., 1999; Leisti et al., 2006; Taraborelli et al., 2010; Kim et al., 2013). Concerning the former issue, even though the total annual TP loading has significantly decreased from 3.5 kg P km^{-2} d^{-1} between 1972 and 1986 to 2.5 kg P km^{-2} d^{-1} between 1987 and 2001 (Minns et al., 2004), it still represents a major regulatory factor of the local water quality problems (Kim et al., 2013). Notably, recent empirical evidence suggests that the potential magnitude of the TP contribution from the ungauged subwatersheds as well as the direct storm sewer discharges have been underestimated, which in turn poses significant challenges in obtaining credible modeling tools and subsequently establishing achievable delisting criteria (Kim et al., 2013). Casting doubt on the reliability of existing modeling exercises in the area, Kim et al. (2013) argued that the likelihood of a substantial underestimation bias in the exogenous loading may lead to a situation, in which two errors (underestimation of the exogenous and overestimation of the internal loading) cancel each other out and result in a misleadingly satisfactory model fit. Recognizing this uncertainty, the same study showed that the response of the bay could vary significantly depending on the assumptions made about the relative importance of the exogenous versus endogenous loading. In this regard, Arhonditsis et al. (2016) concluded that the verification (or further refinement) of the existing loading estimates and subsequently the consolidation of their connection with the prevailing conditions in the historical monitoring sites is perhaps the most critical knowledge gap for identifying the best management practices in the area.

In this study, we use several exploratory techniques to understand the relationships between TP dynamics, such as loading, net export, yield, and concentrations from point and non-point sources, and watershed attributes, including land use cover and morphology of the Bay of Quinte watershed. First, dynamic linear modeling is applied to assess temporal trends in the flow rates in five major tributaries of the area. Second, we develop linear regression models to evaluate their capacity to depict the relationships between TP loading and landscape characteristics of the watershed. We then use self-organizing map (SOM) analysis, a novel pattern-recognition algorithm specifically designed to reduce the multi-dimensionality of environmental datasets and to allow for simpler visualization (and interpretation) of complex patterns (Giraudel and Lek, 2001; Park et al., 2014; Ha et al., 2015). Specifically, SOM is used to elucidate the spatial patterns of land use cover and landscape features and subsequently to identify linkages with the corresponding TP variability. The lessons learned from this study will be used to validate a watershed modeling exercise that intends to improve the annual nutrient loading estimates, to quantify the loading from ungauged subwatersheds, to delineate "hot spots" where excessive nutrient export occurs, and to identify sites that need to be studied more intensively.

Methods

Data description

The total catchment area of the Bay of Quinte watershed is approximately 18,604 km^2. We obtained a land cover database produced by the Ontario Ministry of Natural Resources from satellite remote sensing imaging (available at http://www.geobase.ca/). The original land cover data consisted of 12 subcategories of land use: forest (deciduous and coniferous trees), water (lakes and ponds), wetland (fen, marsh, alvar, bog, coniferous swamp, and deciduous swamp), and other land use types (mining and cutovers) (Fig. 1a). To quantify watershed morphological characteristics, we obtained a 7.2-m digital elevation model (DEM) of Ontario, created by Natural Resources Canada, and used it to calculate the slope of the landscape from the DEM. Soil hydraulic conductivity (K_{sat}) and soil bulk density (BD) were collected from the national soil database (Agriculture and Agri-Food Canada, http://sis.agr.gc.ca/). We used a commercial software package of geographic information system (GIS), ArcGIS 9.3 (ESRI, 2004), for all the relevant calculations.

Water quality monitoring stations are from the Provincial Water Quality Monitoring Network (PWQMN) administrated by the Ontario Ministry of the Environment and Climate Change. From 1998 to 2009, monthly TP concentration data were available at the 73 monitoring stations in the Bay of Quinte watershed. We delineated catchment areas (i.e., unit subwatersheds) using each PWQMN monitoring site as a pour point in GIS. Namely, 73 subwatersheds—that is, gauged watersheds—were created, under the assumption that the corresponding PWQMN stations were drainage pour points. Subwatersheds in which no monitoring stations were located were regarded as ungauged watersheds and their delineation was based on the consideration of the corresponding tributary mouths as drainage pour points (Fig. 1b). We used the Water Survey of Canada (WSC) Program, managed by Environment and Climate Change Canada (Water Survey Division, Burlington, Ontario), to determine daily river/stream inflows for 48 monitoring stations from five major tributaries: the Trent River, Moira River, Salmon River, Napanee River, and Wilton Creek (Fig. 1c and Electronic Supplementary Material (ESM) Table S1). Mean annual TP loads were estimated as the product of mean annual TP concentrations and mean annual flow rates at the 73 PWQMN stations (Moatar and Meybeck, 2005). Because the sampling locations of flow and TP measurements were different, we estimated the mean annual flow rates of the 73 PWQMN stations via a catchment area regression model (Kim et al., unpublished data). The mean annual TP concentrations were derived from daily PWQMN TP data within each year. We also compared the derived TP loads with the Beale-ratio estimates (Preston et al., 1989). We used contemporaneously measured data for concentrations and flow rates (Station ID: 02HJ001 in Table S1 and 17002103802 in ESM Table S2). The loading estimates between two methods were almost identical. We also calculated mean annual point TP loading as the product of mean annual TP concentration and effluent flow, based on 26 STPs within the Bay of Quinte watershed (Ontario Ministry of the Environment and Climate Change, Eastern Region, Kingston). In addition to TP loading, we calculated net TP export by subtracting upstream and downstream TP exports. We also estimated TP yield as the net TP export divided by the area of each subwatershed. The number of septic tanks in the Bay of Quinte watershed was based on the assumption that each household in an un-serviced area has one septic tank (Statistics Canada, http://www.statcan.gc.ca/).

Dynamic linear modeling

Dynamic linear modeling (DLM) analysis was used to detect the temporal trends of the daily flow rates, for the five tributaries identified above, while explicitly accounting for their covariance with the precipitation. Although DLMs have a simple structure similar to conventional linear regression models, their benefits are the time-variant parameters along with their capacity to provide forecasts influenced by recent, rather than distant, data (Pole et al., 1994; Lamon et al., 1998; Stow et al., 2004). DLM forecasts for the response variable at time t are based on contemporaneous observations and prior knowledge of the parameters. Based on iterative applications of Bayes' theorem, our knowledge with respect to the parameter values is sequentially updated, using the data obtained at each time step and prior information to derive the parameter posteriors. This evolving nature offers greater insights into cause–effect relationships, and thus enables unraveling complex ecological patterns over time (Mahmood et al., 2013). All

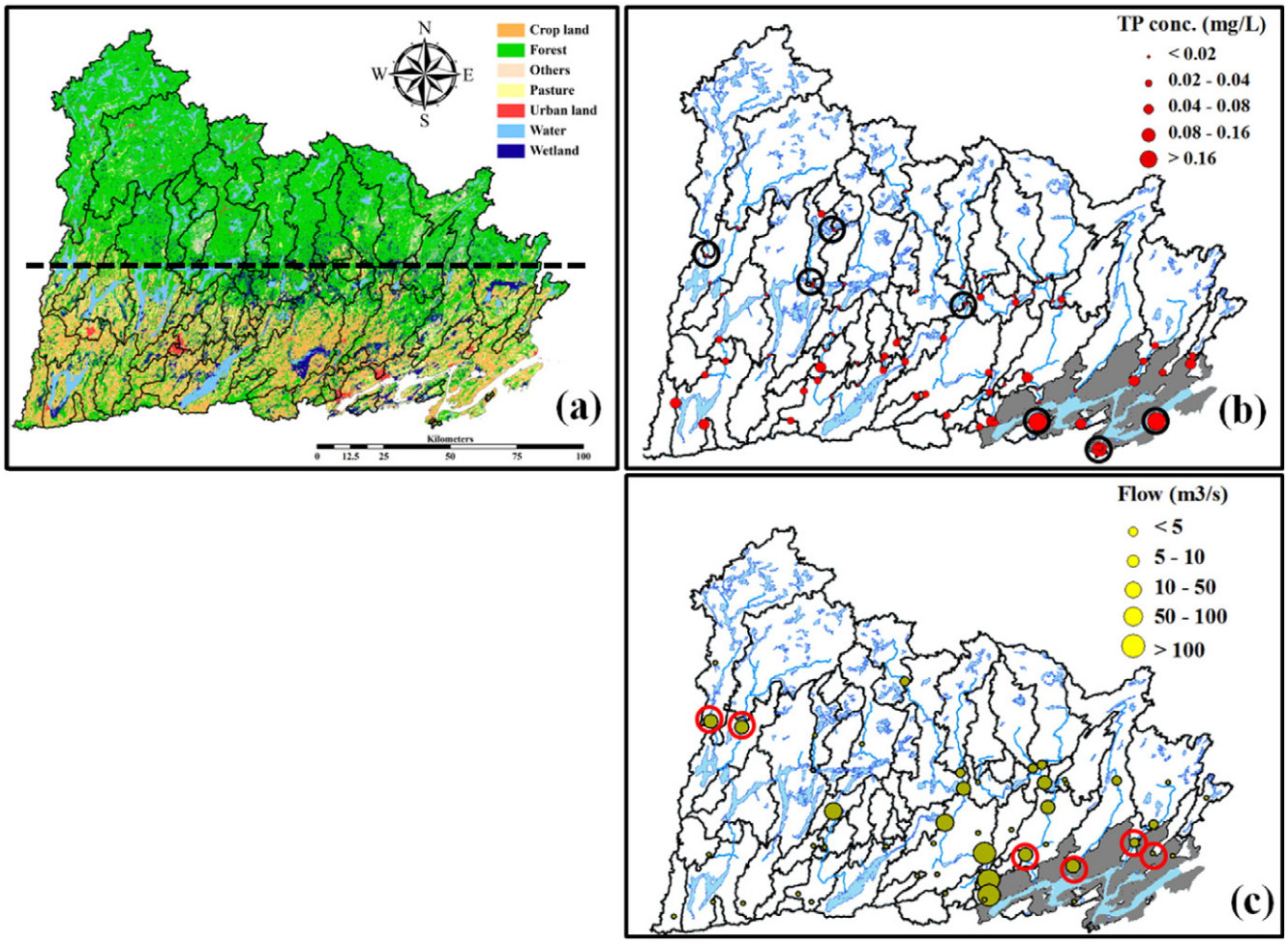

Fig. 1. General patterns of data available in the Bay of Quinte watershed: (a) land use coverage: the dashed line indicates the southern geological boundary of the Canadian Shield, (b) TP concentrations measured at 73 water quality monitoring stations, and (c) flow rates recorded at 48 monitoring stations. The circled sites indicate seven PWQMN stations (Gull River, Mississauga River, Lake Anstruther, Crowe River, Sawguin Creek, Marsh Creek, and Cressy Creek from left to right in panel (b) and six flow-monitoring stations used for DLM (HF002, HF003, HL001, HM003, HM007, and HM004 from left to right in panel (c). The areas delineated by solid lines are gauged subwatersheds, while those with gray color are ungauged watersheds.

DLMs comprise an observation equation and system equations as follows:

Observation equation:

$$\ln[flow]_{tk} = baseline\ flow_t + \beta_t \cdot \ln[rain]_{tk} + \psi_{tk} \qquad \psi_{tk} \sim N[0, \omega_t]$$

System equations:

$$baseline\ flow_t = baseline\ flow_{t-1} + rate_t + \varepsilon_{t1} \quad \varepsilon_{t1} \sim N[0, \sigma_{t1}]$$

$$rate_t = rate_{t-1} + \varepsilon_{t2} \qquad \varepsilon_{t2} \sim N[0, \sigma_{t2}]$$

$$\beta_t = \beta_{t-1} + \varepsilon_{t3} \qquad \varepsilon_{t3} \sim N[0, \sigma_{t3}]$$

$$\omega_t^{-2} = \gamma^{t-1} \cdot \omega_1^{-2}, \ \ \sigma_{tj}^{-2} = \gamma^{t-1} \cdot \sigma_{1j}^{-2} \quad t > 1, j = 1 \text{ to } 3$$

$$baseline\ flow_1, rate_1, \beta_1 \sim N[0, 10000] \quad t = 1$$

$$\omega_1^{-2}, \ \ \sigma_{1j}^{-2} \sim Gamma(0.001, \ \ 0.001)$$

where $\ln[flow]_{tk}$ is the observed river flow at year t and day k; $\ln[rain]_{tk}$ is the corresponding precipitation, both expressed in natural logarithmic scale; $baseline\ flow_t$ is the annual average flow; $rate_t$ is the rate of change of annual flow; β_t is the precipitation (regression) coefficient; ψ_{tk} and ε_{tj} denote stochastic error terms for year t sampled from normal distributions with zero means and variances ω_t and σ_{tj}, respectively; the discount factor γ represents the aging of information with the passage of time. In this study, we postulated that 5% of the information, contained in the data, is lost with each time step (Lamon et al., 1998; Stow et al., 2004). In addition, the stochastic nodes *baseline flow*, *rate*, and β for the initial year ($t = 1$) follow a normal distribution with mean 0 and variance 10,000, whereas ω_1^{-2} and σ_{1j}^{-2} are determined by gamma distributions with shape and scale parameters of 0.001, indicating that our prior knowledge is "non-informative" or vague. To maximize the signature of precipitation to river flow, we implemented cross-correlation analysis based on different moving time windows and chose the one for each of the examined tributaries with the highest correlation coefficient.

Self-organizing map

Self-organizing map (SOM), a form of Artificial Neural Network analysis, is recognized as a powerful means of extracting information from complex, multi-dimensional data and mapping them onto reduced dimensional space. The SOM network, originally proposed by Kohonen (1982), mimics the intellectual functioning of higher animal brains, whereby the neurons (i.e., data vectors) compete with one another in Euclidean map space, thereby converting highly nonlinear relationships into simple geometric relationships. Kohonen (1997) stressed that SOM, trained by purely nonlinear networks, could be more powerful

in processing very complex and intricate problems, in contrast to conventional clustering and classification methods. SOM has been widely applied to pattern recognition of various learning problems, and it is deemed one of the more robust methodologies, particularly due to its convenience for visual understanding (Chon et al., 1996). Counter to linear ordination methods, including principal component analysis and correspondence analysis, SOM's main advantage is the ability to project multivariate data in a nonlinear way. SOM also differs from conventional methods in that, in order to maintain the topological features of the input array, it operates on mechanistic principles of biology, such as competition and adaptation in data learning processes. Thus, SOM is more effective not only in converting high-dimensional constructs to lower dimensional configurations, but also in clustering essential features of complex nonlinear data (Giraudel and Lek, 2001).

SOM's network architecture is composed of two layers, input and output (see Glossary of Terms at end of this article). The connectivity between input and output layers is defined as arbitrary random weight vectors in the initial stage. While the data are trained in the network, the distances between input and weight vectors are compared. Among them, one neuron (i.e., weight vector) that has the shortest distance to the input vector is designated the best matching unit (BMU). Subsequently, all the weight vectors are updated and adjusted according to topology of the BMU, until all the neurons become stabilized over time. During this learning process in which the "*nonlinear projection*" is formed, all nodes of the weight vectors activate and resemble each other in similar locations (or topography). This will result in "*a local relaxation or smoothing effect*" of the weight vectors of neurons in the neighborhood and will lead to "*global ordering*" in continued learning (see p.109–115 of chapter 3, Kohonen, 1997). The primary equations of SOM are expressed as follows:

$$|x-\omega_{BMU}| = \min_i |x-\omega_i|$$

$$\omega_i(t+1) = \omega_i(t) + h(t)\cdot d_i(t)$$

$$h(t) = \alpha(t)\cdot \exp\left(-\frac{|\omega_{BMU}-\omega_i|^2}{2\sigma^2(t)}\right)$$

whereby $d_i(t)$ represents a minimum Euclidean distance between input x and weight ω in the i number of individual nodes (i.e., identical to the size of SOM) at time t. In the relaxation process, the neighborhood function $h(t)$ plays a key role as a smoothing kernel defined over the SOM lattices (see Glossary below). For convergence, $h(t) \to 0$ while time $t \to \infty$; both the learning-rate factor $\alpha(t)$ and the *BMU*-coverage width $\sigma^2(t)$ are monotonically decreasing over time.

For the SOM analysis, we used 18 input variables, including three morphological characteristics (slope of landscape, soil hydraulic conductivity, and soil bulk density) and 15 forms of land use cover (lake, pond, alvar, bog, coniferous swamp, deciduous swamp, fen, marsh, deciduous forest, coniferous forest, cutover, mining area, urban land, pasture, and cropland) in the Bay of Quinte watershed (Table S2). The extent of coverage of each land use type was expressed as an areal percentage within each subwatershed. Subsequently, the SOM was trained using 210 data samples—encompassing 73 gauged and 137 ungauged subwatersheds of the bay—and distributed these data onto two-dimensional hexagonal lattices. The node number of the output layer (i.e., SOM size) was determined based on the value close to $5\sqrt{n}$ proposed by Vesanto and Alhoniemi (2000). Data ordination of the output layer was classified by a hierarchical cluster analysis, according to similarities of the corresponding weight neurons. To identify each cluster's most dominant features, we compared the average of land use coverage and morphological characteristics among the clusters and then, within each cluster, we linked these averages to TP loading variables, such as mean annual point-source loading, net export, yield, and concentration. For all these analyses, we used the SOM Toolbox developed by the Helsinki University of Technology (Vesanto et al., 2000).

Results–Discussion

General watershed characteristics and flow patterns in the major tributaries

The Bay of Quinte watershed is geographically separated into two major areas: the northern basin set on the Canadian Shield and the southern basin. The geological substrate of the northern basin mainly consists of igneous rock and the landscape is dominated by boreal forests (Fig. 1a). Thus, this area remains mainly pristine and is subject to minimal release of phosphorus loads through erosional processes. Consequently, the measured TP concentrations in the creeks of the northern basin are fairly low (<20 μg L^{-1} vis-à-vis an average of 30 μg L^{-1} over the entire watershed), especially at Lake Anstruther (6 μg L^{-1}), Mississauga River (7 μg L^{-1}), Gull River (8.8 μg L^{-1}), and Crowe River (9.6 μg L^{-1}) (Fig. 1b). By contrast, the southern basin is mainly characterized by agricultural land uses, such as croplands and pastures (Fig. 1a). In addition, urban areas have sprawled in the lower basin in concert with developing cities and big towns, such as Peterborough, Trenton, and Belleville. For these reasons, distinctly higher TP concentrations are found in the lower part of the watershed, particularly at Sawguin Creek (231 μg L^{-1}), Cressy Creek (176 μg L^{-1}), and Marsh Creek (138 μg L^{-1}). Regarding the spatial pattern of river/stream flows, the flow rates recorded were distinctly higher in the Trent River than in other tributaries (Fig. 1c and Table S1). Except for the mean flow rates, we also examined within-year and year-to-year flow variability in various gauged locations, as it represents a critical factor that shapes the uncertainty of TP loading from the Bay of Quinte watershed. The three highest coefficient of variation (CV) values were similarly found in the Trent River catchment, e.g., 52.8% at Blackstock Creek in the upper Trent River basin (station ID 02HG003, ESM Fig. S1), which primarily stem from the slope of landscape and soil texture. Steeper slopes are apt to induce rapid runoff and greater sediment and phosphorus loss rates (Soldat and Petrovic, 2008). Soil texture (e.g., loam, silt, clay, and sand) is closely associated with soil hydraulic conductivity and permeability, which can then modulate infiltration rates and land-to-stream phosphorus delivery (Djodjic et al., 2004; van Es et al., 2004).

DLM analysis of the flow rates focused on four key results: (*i*) the temporal trends of mean annual flow rates; (*ii*) annual changes in flow rates; (*iii*) the slope coefficient β, representing the strength of the relationship between flow rates and precipitation; and (*iv*) percentage of annual flow rate change ($[Flow_{year} - Flow_{year\text{-}1}]/[Mean\ Annual\ Flow] \times 100$) in the Trent River (station ID: HF002 and HF003), Moira River (*HL*001), Salmon River (HM003), Napanee River (HM007), and Wilton Creek (HM004), respectively (Fig. 2; Table 1). In Trent River 1 (HF002), the covariate of flow at day t was the moving average of the precipitation occurring over the six antecedent days (i.e., average from $rain_t$ to $rain_{t\text{-}6}$), while a 4-day moving window of precipitation was used in Trent River 2 (HF003, Fig. 1c). When accounting for the covariance with precipitation, the projected annual average flow rates have been larger in Trent River 1 (≈20 m^3 s^{-1}) than in Trent River 2 (≈10 m^3 s^{-1}) over the past 40 years (1965–2005). In both locations, annual changes of the flow rates were positive but significantly decreased from the 1960s to the mid-1970s (right-top of Trent River 1 and 2 in Fig. 2), that is, the tributary flow was increasing with decreasing rates. The flow rates in both locations have (on average) stabilized thereafter (1980–2005) but were subject to year-to-year variability as demonstrated by the short-term shifts between positive and negative annual flow rate changes. Interestingly, the two predominantly forested subwatersheds showed different patterns with respect to the time-variant regression coefficient β_t, which in turn suggests differences in the influence of precipitation on flow rates. In Trent River 2, the slope

was three times higher and gradually increased relative to Trent River 1. By contrast, β_t of Trent River 1 was lowest among all the tributaries of the Bay of Quinte watershed, and this value was practically equal to zero in 1988, indicative of a very weak flow–precipitation relationship during that year. The latter pattern likely stems from the fact that the flow records in Trent River 1 monitoring station are closely related to a series of dam operations at Gull River, and therefore the upstream regulations result in more stable flow rates that are weakly connected with daily precipitation. On the other hand, Burnt River (Trent River 2), though regulated, is not to the degree of Gull River, and therefore is subject to greater temporal variability and tighter relationship with precipitation.

Regarding the other tributaries, we found that a 6-day, 3-day, 8-day, and 3-day moving window of precipitation had the strongest signature on flow rates in Moira River, Salmon River, Napanee River, and Wilton Creek, respectively (Table 1). These results indicate that hydrological response—that is, the translation of precipitation into runoff—is fastest in Salmon River and Wilton Creek, whereas Moira River, and Upper Napanee River also have some flow regulation, though not to the degree of Trent River. All these tributaries in question, including Salmon River and Wilton Creek, have historically shown more fluctuating flow patterns than in Trent River (left-top in Fig. 2). Until the late 1980s, annual change of flow rates was decreasingly positive in Moira and Napanee Rivers. Since then, these rates have become quite stable in Napanee

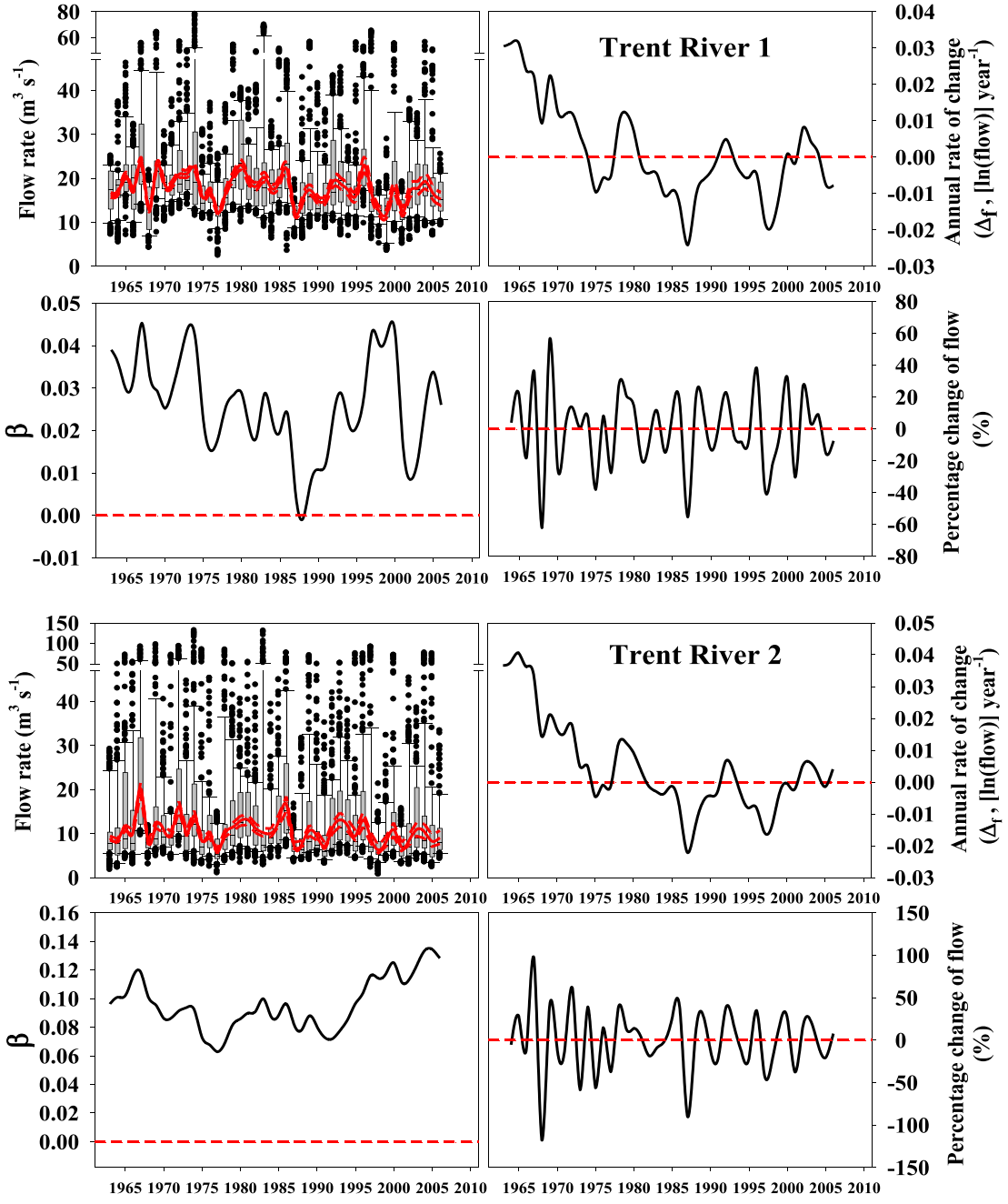

Fig. 2. DLM analysis of the temporal trends of flow rates in five tributaries of the Bay of Quinte watershed; Trent River upstream 1, Trent River upstream 2, Moira River, Salmon River, Napanee River, and Wilton Creek. *Top-left* panels for each river depict the mean annual flow rates when accounting for the covariance with precipitation (red solid line: mean values, dash lines: 95% posterior predictive intervals, box plots: observed data). *Top-right* panels for each river depict the annual rates of change of the flow rates. *Bottom-left* panels for each river depict the slope regression coefficient of precipitation in response to flow rates. *Bottom-right* panels for each river depict percentage change of flow.

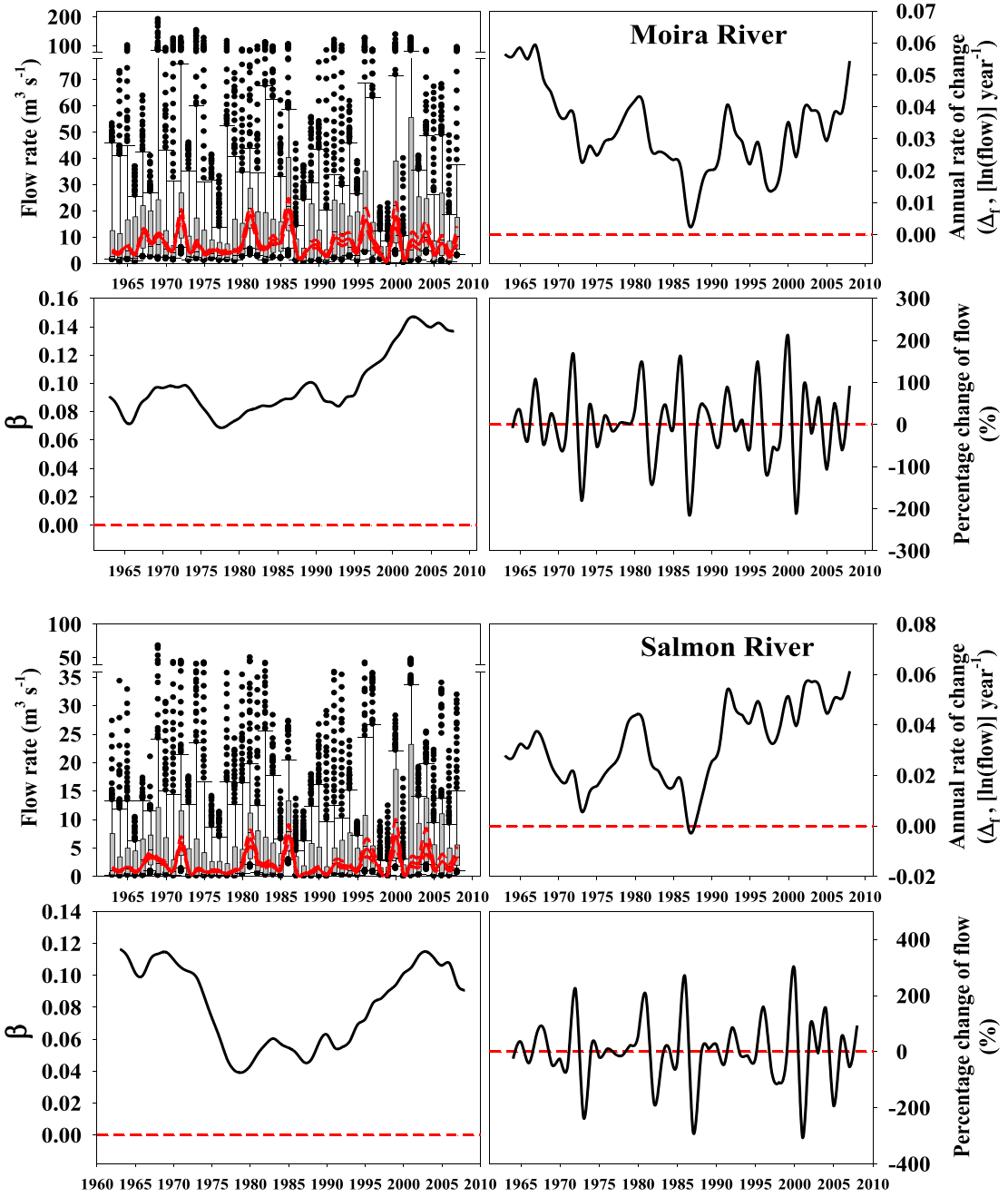

Fig. 2 (*continued*).

River, whereas they have gradually increased in Moira River (right-top in Fig. 2). Annual changes of flow rates in Salmon River and Wilton Creek have shown a pattern of gradual increase over the entire period (1965–2010). Specifically, the annual change of flow rate was mostly negative in Wilton Creek until 2007, i.e., the flow was decreasing with a slowing rate, but more recently has become positive. The slope coefficient β_t was mostly stable, except in Salmon River, until 1990. But since 1990, the coefficient has continuously increased in Moira River and Salmon River (left-bottom in Fig. 2). Perhaps this increasing pattern of β_t is related to expanding urbanization at Moira River (and partially at Salmon River) near Belleville. Urbanization can accentuate the impact of storm events, resulting in more dynamic ("flashy") hydrographs relative to less disturbed streams (Duan et al., 2012), as well as significant increases in annual flow rates, dry-season runoff, and flood magnitudes (White and Greer, 2006). Moreover, the increasing degree of imperviousness of the land surface, resulting from urban sprawl, plays a key role in shaping the buildup and washoff processes when storm events occur (Butcher, 2003). With respect to Wilton Creek, β_t has been steadily high over the 40-year study period. The latter is a typical small-drainage stream, where runoff processes are generally triggered more promptly from precipitation events (Minns et al., 1986b; McGlynn et al., 2004). Mean annual flow rate (0 ~ 0.5 $m^3 s^{-1}$) in Wilton Creek has been significantly smaller than in the other tributaries. Percentage of annual flow change has been lower in Trent River than in other tributaries (average: ≈25% in Trent River, ≈70% in Moira River, ≈80% in Salmon River, ≈50% in Napanee River, and ≈75% in Wilton Creek). Except for the Trent River, larger fluctuations have been recorded in the tributaries in recent years. In particular, the highest percentage (≈300%) was recorded in Wilton Creek in the early 2000s (right-bottom in Fig. 2).

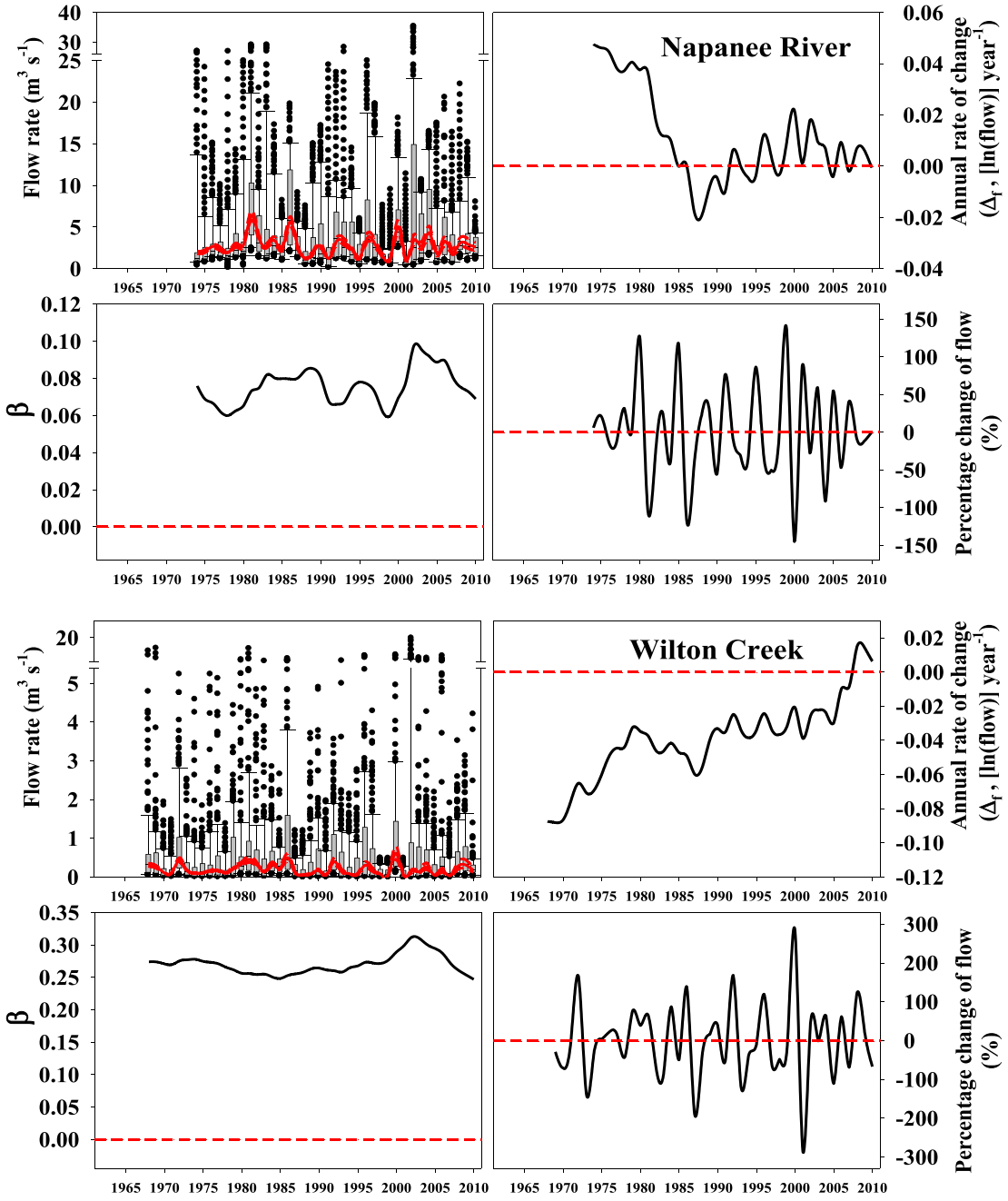

Fig. 2 (*continued*).

Table 1
Areal coverage of different land uses in the six gauged subwatersheds used for our dynamic linear modeling analysis.

Basin	Unit	Lake	Crop land	Urban land	Conifer forest	Deciduous forest	Pasture	Alvar	Bog	Fen	Swamp	Marsh	Logging	Mining
Trent1	km^2	216.9	7.2	8.8	358.4	699.1	25.0		18.5	1.1	3.4	0.1	9.7	3.2
	%	16.0	0.5	0.7	26.5	51.7	1.9	0.0	1.4	0.1	0.3	0.0	0.7	0.2
Trent2	km^2	62.2	68.7	0.1	195.7	112.0	55.3	15.7	2.7		21.1	0.6		0.0
	%	11.7	12.9	0.0	36.6	21.0	10.4	2.9	0.5	0.0	3.9	0.1	0.0	0.0
Moira	km^2	129.0	261.7	11.8	991.7	844.1	143.0	2.6	34.3	6.7	215.6	3.0	7.7	96.3
	%	4.7	9.5	0.4	36.1	30.7	5.2	0.1	1.2	0.2	7.8	0.1	0.3	3.5
Salmon	km^2	52.0	77.5	0.6	311.5	215.6	69.8	34.9	17.5	4.5	50.0	2.5	6.2	67.5
	%	5.7	8.5	0.1	34.2	23.7	7.7	3.8	1.9	0.5	5.5	0.3	0.7	7.4
Napanee	km^2	70.1	128.8	3.5	100.0	320.2	86.0	16.5	3.3	7.9	51.0	9.7	0.0	7.6
	%	8.7	16.0	0.4	12.4	39.8	10.7	2.1	0.4	1.0	6.3	1.2	0.0	0.9
Wilton	km^2	0.3	38.8		10.6	22.1	25.6	4.8		0.2	1.0	0.1		0.9
	%	0.3	37.2	0.0	10.1	21.1	24.6	4.6	0.0	0.2	0.9	0.1	0.0	0.9

Relationships between total phosphorus export and land use

Both agricultural and urban nutrient export fluxes are highly variable and contingent upon a number of regulating factors, including soil type, urban storm water management, agricultural intensity, and conservation practices (Moore et al., 2004; Soldat and Petrovic, 2008; Soldat et al., 2009). Agricultural nutrient export rates have historically been considered higher than those from urban areas, although recent empirical and modeling evidence suggests that urban TP loads can be comparable or even higher (Winter and Duthie, 2000; Duan et al., 2012). High urban TP loading has been attributed to storm water-induced bank erosion, high fertilizer use on residential lawns, and lack of phosphorus retention on impervious surfaces (Withers and Jarvie, 2008; Pfeifer and Bennett, 2011). In the same context, considerable insights have been gained by a recent comparative examination of the daily flows in an urbanized (Redhill Creek) and an agricultural (Grindstone Creek) catchment in the neighboring Hamilton Harbour area, which supported the idea of a single threshold separating two states of watershed response to precipitation (Wellen et al., 2014). It was hypothesized that the watershed response to precipitation occurs in distinct states, such that precipitation depth above a certain threshold triggers an extreme state, which is characterized by a qualitatively different response of the watershed to precipitation. To solidify this working hypothesis, Long et al. (2014, 2015) have collected 87 24-h level-weighted composite samples from a variety of catchment states (rain, snowmelt, baseflow) from all four major tributaries to Hamilton Harbour between July 2010 and May 2012. The key findings from this research were as follows: (*i*) daily TP loads varied by three orders of magnitude between wet and dry conditions, with storm events and spring freshets driving peak daily loads in urban and agricultural watersheds, respectively; (*ii*) areal TP loads were significantly higher from the urban relative to the agricultural watersheds; and (*iii*) the characterization of TP concentrations during high flow conditions was essential in establishing accurate concentration versus flow relationships and subsequently nutrient load estimates. The brief, but intense, events which occurred <10% of the time were found to be responsible for 50%–90% of TP loads delivered to Hamilton Harbour from its tributaries. While the lessons learned from the integrated watershed-receiving waterbody system in the Hamilton Harbour AOC are typically used to draw inference about the Bay of Quinte AOC and vice versa, the question arising here is to what extent some of the previously mentioned patterns of agricultural versus urban nutrient export fluxes hold true in the Bay of Quinte watershed.

In particular, TP loads exhibited a spatial gradient from the upper to the lower basin, but the corresponding standard deviations (i.e., year-to-year variability) did not demonstrate a clear pattern (Fig. 3). TP loads from upstream catchments were distinctly lower than those from downstream catchments, and the highest TP load values were found in the lower part of the Trent River with the largest drainage area among the major local tributaries (Fig. 3a). Specifically, large annual TP loads, exceeding 4 ln P tons yr^{-1} ($\approx$55 P tons yr^{-1}), were frequently found in the catchment between Peterborough and Trenton. In this region, TP loads are partly elevated as a result of point-source loading emanating from the nearby urbanized areas. Concerning variability in annual TP loading, we found larger standard deviations primarily in locations where the stream order was lower, which was consistent with our DLM analysis showing greater year-to-year variability in the flow rates in small streams. In a similar manner, we found that subwatersheds with higher TP load variability were geographically close to stations in which variability of flow rates was also high (Table S2). For instance, the subwatershed of ID 108 is quite close ($\approx$20 km) to the flow-monitoring station (02HG003) that showed the largest CV of flow rate (ESM Fig. S1). Given that the two contiguous locations have similar morphological characteristics, it is reasonable to assume that the relationship between TP loading and flow rate is significantly strong. Nonetheless, it is also worth mentioning that agricultural land also occupies the largest portion (32.6%, 13.35 km^2) of this subwatershed (ID 108 in Table S2 and Fig. S1), and therefore TP export from the agricultural land may also be modulated by different land use/management practices, such as crop types and tillage methods.

In order to compare in greater depth TP export, we first examined TP yield (mass per unit area per time) and net TP export (mass per time) with respect to the presence of a particular land use type in each of the 73 gauged subwatersheds (Fig. 4). If we do not consider the actual area occupied by the different land use types, the general patterns of TP yield and net TP export suggest the largest amounts of phosphorus originate from subwatersheds that have croplands, pastures, or forests. TP yield was greatest in subwatersheds with croplands (mean: 29.7 kg km^{-2} yr^{-1}, median: 6.0 kg km^{-2} yr^{-1}), followed by forests (mean: 14.2 kg km^{-2} yr^{-1}, median: 6.1 kg km^{-2} yr^{-1}) and pastures (mean: 9.2 kg km^{-2} yr^{-1}, median: 2.5 kg km^{-2} yr^{-1}). Net TP export was larger in subwatersheds with forests (mean: 1.25 tons yr^{-1}, median: 0.58 tons yr^{-1}) than in croplands (mean: 1.01 tons yr^{-1}, median: 0.48 tons yr^{-1}). Interestingly, net TP export and yield were significantly lower in urban sites, which deviates from the emerging paradigm that TP

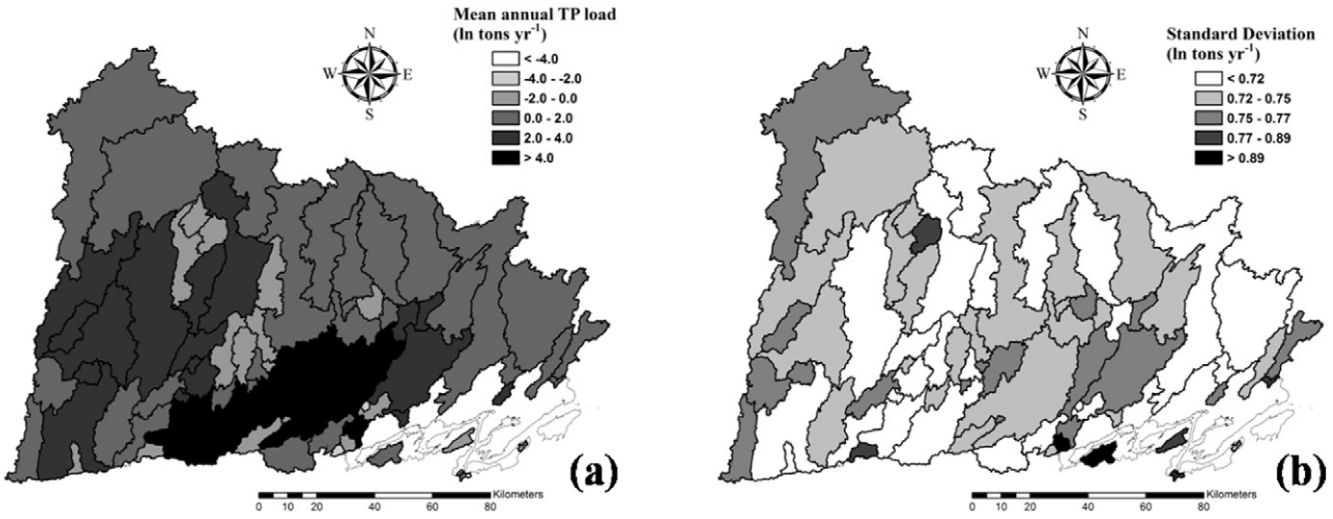

Fig. 3. TP loadings measured at 73 PWQMN stations in the Bay of Quinte watershed; (a) mean annual *TP* loadings and (b) standard deviation of annual *TP* loadings.

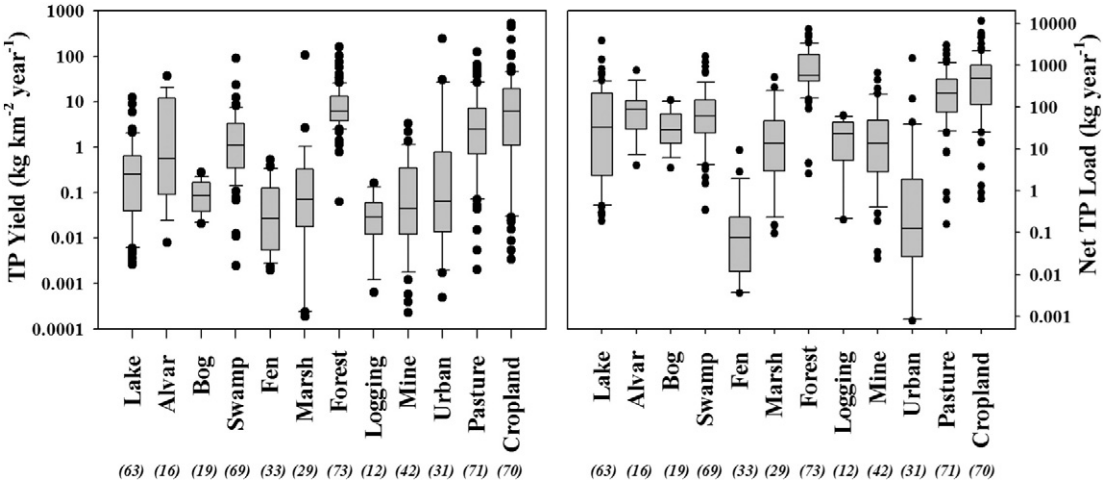

Fig. 4. TP yield (left) and net *TP* load (right) according to land use types in the Bay of Quinte watersheds. Bracketed numbers indicate the number of subcatchments that each land use type is found regardless of the actual area occupied.

export tends to be higher in urban/suburban lands than in forest and agricultural areas (Duan et al., 2012). Nonetheless, the latter finding should be viewed with caution as the fractional areas (%) of urban lands within each subwatershed are usually much smaller than those of croplands. Thus, the corresponding box plots do not fully reflect the relationship between TP yields/net exports and urban land, as they are confounded by the impact of other land uses that occupy larger areas in the 31 subwatersheds, where urban sites are also found. To shed light on the latter issue, we examined the relationships between annual net TP export and actual area occupied in each subwatershed by six land uses: lake, wetland, forest, urban land, pasture, and cropland (Fig. 5). Box–Cox power transformations were implemented to stabilize variance of data and effectively linearize the bivariate relationships examined (Box and Cox, 1964; see ESM Fig. S2). Based on the corresponding slope values, cropland (0.29) was most strongly related to net TP load (or net TP export), followed by pasture (0.25), wetland (0.24), lake (0.14), forest (0.13), and urban area (0.06). Similar to the previous results though, the area occupied by urban environment was not a strong predictor of the net TP loading. Further, the coefficient of determination values of the corresponding simple regression models were fairly low (r^2 = 0.003 ~ 0.20). The relationship between annual net TP export and percentage areal coverage for each land use was also found consistently weak (ESM Fig. S3), and therefore the use of methods that stipulate linearity may not be adequate to elucidate the relationship between TP loading and land use patterns in the Bay of Quinte watershed.

Land use pattern recognition using SOM

The SOM produced a total of 18 hexagonal lattice maps, visualizing the relative topological distribution of input variables used in the data learning process. Fig. 6 demonstrates two-dimensional distributions of the 18 input variables on SOM, as depicted by chromatic contrast. The dark color represents large values or high densities of corresponding inputs (or variables). Notably, a higher degree of slope appears at the upper part of SOM. A similar pattern of high densities at the upper areas of the 2D maps is also found for deciduous and coniferous forests, bogs, logging, and mining areas. This similarity reflects the (plausibly) strong correlation between the slope of the landscape and the areal extent of these land use types in the Bay of Quinte watershed. Along the same line of thinking, we also found that K_{sat} is inversely correlated with the soil bulk density. The SOM pattern of bogs is clearly different from those of other types of wetlands, such as alvar, coniferous and deciduous swamps, fen, and marsh. By contrast to K_{sat}, soil bulk density and wetlands, pasture, and cropland have higher density over the lower part of SOM, while urban land is localized in a small areal range. The urban land areas partly resemble the SOM density patterns of ponds.

The Bay of Quinte watershed was also visualized based on SOM data classification, representing heterogeneous patterns of land use and morphological characteristics (left panels in ESM Fig. S4). Data inputs from each subwatershed correspond to each of the hexagonal lattices (right panels in ESM Fig. S4). Using all data of land use and other attributes, covering a total 210 subwatersheds (i.e., 73 gauged and 137 ungauged ones), SOM classified the Bay of Quinte watershed into six distinct clusters (Fig. 7). Table 2 shows total average and cluster average values of 18 input variables (from 210 subwatersheds) and observed TP dynamics (from 73 gauged subwatersheds). In Cluster 1, where specific types of wetlands demonstrate their highest percentage areas (≈9.8% of alvar, ≈8.1% of coniferous swamp, and ≈0.43% of fen) among the six clusters, point-source loading is low (30 kg yr^{-1}) and net TP export in particular is the smallest (1.08 tons yr^{-1}). In Cluster 2, landscape slope is largest, soil bulk density highest, and forest coverage (i.e., deciduous and coniferous area) also highest. The mining and logging areas are the most abundant, which is typical of the Canadian Shield's mountainous regions. In the same cluster, TP yield and TP concentration are the lowest (8 kg km^{-2} yr^{-1} and 14 μg L^{-1}, respectively) across all six clusters. In Cluster 3, most subwatersheds are located near the Bay, cropland coverage is highest (≈75%), and annual TP yield and average TP concentration are the highest (528 kg km^{-2} yr^{-1} and 103 μg L^{-1}). In Cluster 4, K_{sat} is the highest, deciduous swamp is most abundant, and cropland coverage is second largest (≈41%). The subwatersheds in Cluster 4 experience the largest net TP export, which is primarily derived from their larger areal extent, along with larger (i.e., the second largest) fractions of cropland. In Cluster 5, urban land occupies ≈74% of the subwatersheds, although urban sites are relatively small and fragmented. Net TP export and yield are second highest (3.72 tons yr^{-1} and 209 kg km^{-2} yr^{-1}), together with largest point-source loading (2.44 tons yr^{-1}). The subwatersheds classified in Cluster 5 include the towns of Peterborough, Trenton, and Belleville. In Cluster 6, pasture and cropland occupy ≈60% of the land use, marsh density is the highest, and the subwatersheds within the same cluster are located adjacent to the Bay of Quinte, point-source loading and TP concentration are second highest (158 kg yr^{-1} and 69 μg L^{-1}, respectively).

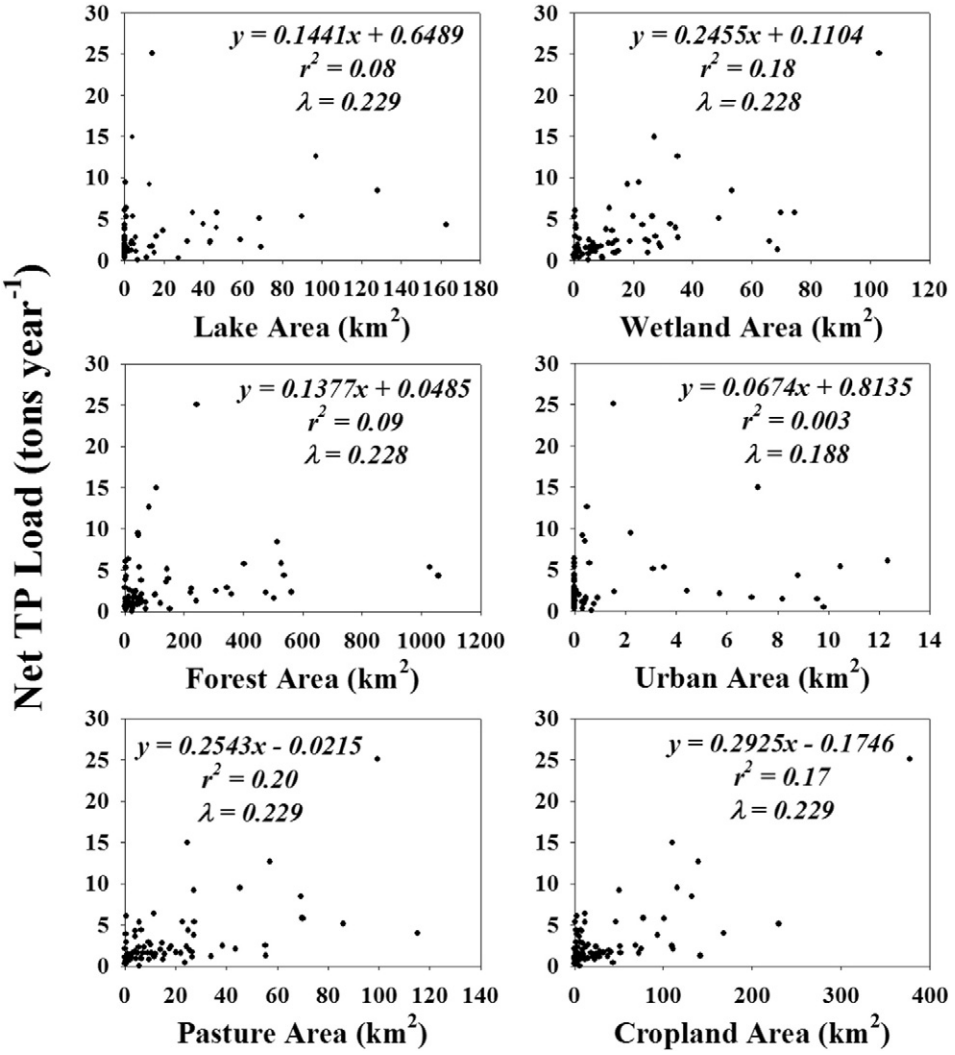

Fig. 5. Relationships between annual net TP exports and different land use areas (lake, wetland, forest, urban land, pasture, and cropland) in the 73 watersheds. The lambda (λ) value indicates the power of the Box–Cox transformation to which all data were raised during the development of regression models.

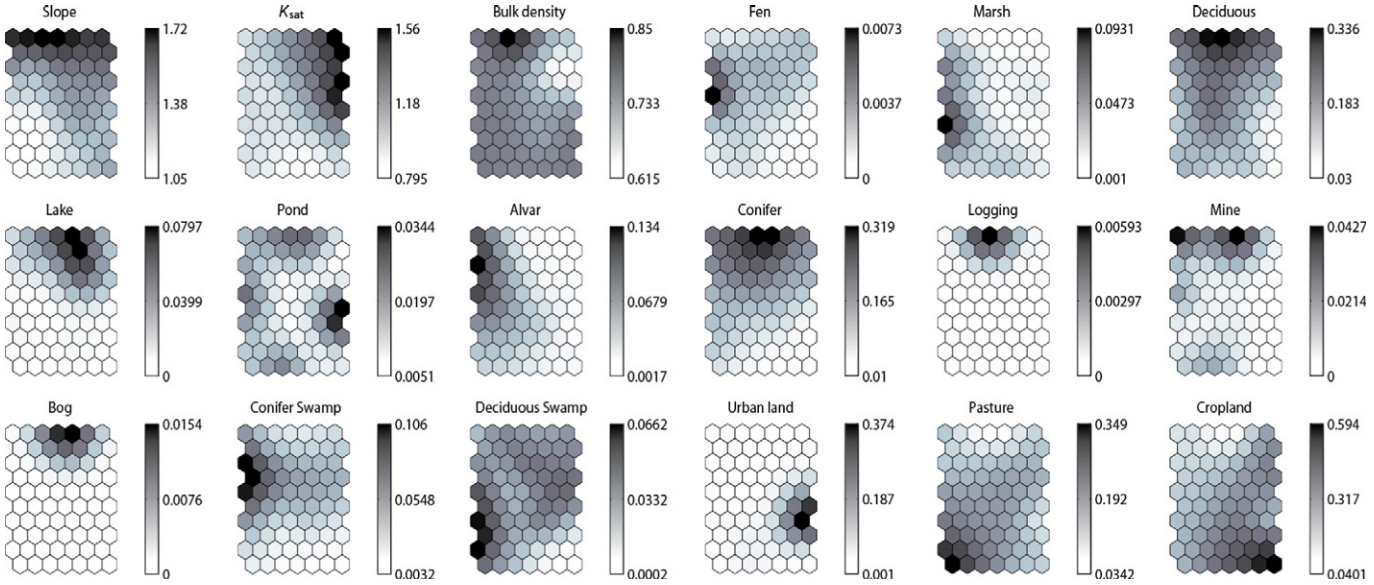

Fig. 6. SOMs of morphological characteristics and land use coverage, which visualize relationships among multi-dimensional data on lower dimensional (2-D) maps. Right bands indicate the range of values of each variable. K_{sat} refers to soil hydraulic conductivity. Units are the same as shown in Table 1.

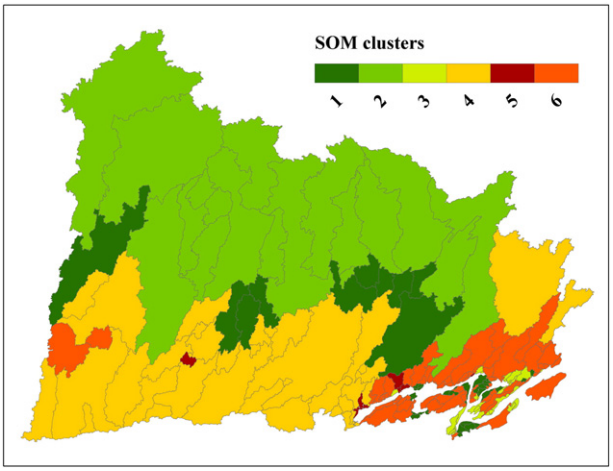

Fig. 7. SOM classification of a total of 210 (73 gauged and 137 ungauged) subwatersheds in the Bay of Quinte. Clustering is based on Fig. S2.

Conclusions

The paradigm of phosphorus, as the primary driver of the severity of eutrophication problems, has profoundly shaped the restoration actions in the Bay of Quinte. Local management strategies were originally designed to reduce phosphorus loading from all major municipal and industrial point sources. Stemming from the reduction of phosphorus in detergents along with the upgrades at the local wastewater treatment plants, daily average phosphorus loadings into the Bay of Quinte decreased from 214 kg P d^{-1} between 1968 and 1972 to 60–68 kg P d^{-1} between 1978 and 1986 and have seldom exceeded the level of 25 kg P d^{-1} since 2000 (Kim et al., 2013). This significant decline in the proportion of phosphorus loading associated with point sources (<3%) has shifted the focus to the contribution of tributaries as an important regulatory factor in determining the trophic status of the downstream water body. While every watershed is unique in terms of the magnitude of tributary nutrient concentrations and prevailing flow conditions, there are several common factors underlying the observed loading variability such as the land use, seasonality, catchment state (baseflow or high flow conditions), and physiographic attributes (Long et al., 2014, 2015). Thus, establishing the causal linkages among land use patterns, morphological characteristics, and non-point-source loading is critical for understanding the current state of eutrophication in the Bay of Quinte. The basic lessons learned from the present analysis are summarized below.

Owing to its robustness in pattern recognition (Chon et al., 1996), SOM delineated six spatial clusters that exhibit dominant land use characteristics, except for Cluster 1 which can be described as depicting transitional areas. The main distinct feature for this cluster was the presence of different wetland types (alvar, coniferous swamp, and fen) with areal coverage higher than in other locations. Cluster 2 is typical of mountainous watersheds, in which both slope of landscape and forest coverage are highest. Cluster 3 contains a high proportion of agricultural land in the vicinity of the Bay of Quinte and is mostly located in the ungauged watershed. Cluster 4 covers the lower part of Trent River catchment, except for two subwatersheds, one located at the upper Napanee River and the other at the upper Wilton Creek. The latter cluster is also characterized by the second largest cropland fraction and the highest hydraulic conductivity values of all clusters. Cluster 5 is primarily characterized by urban areas and the highest areal coverage of ponds, while Cluster 6 includes a high proportion of pasture (≈30%) and also contains a large portion of the ungauged watershed.

Although urban areas are very small and partly isolated in the Bay of Quinte, their impact on TP loads is pronounced, as reflected in Cluster 5's second largest net TP export (3.729 tons P yr^{-1}) and TP yield

Table 2
SOM classification of the watershed attributes in the Bay of Quinte. White-colored variables are input used for data learning, and gray-shaded variables are observed values (mean ± standard error) corresponding to each SOM cluster. Bold numbers indicate the highest value for each variable among the six clusters. Superscripts indicate statistically significant differences in each row/variable among the six clusters based on Scheffe's multiple comparison test ($p < 0.05$).

Variable	Unit	Mean	Cluster 1	Cluster 2	Cluster 3	Cluster 4	Cluster 5	Cluster 6
Slope of landscape	degree	2.792 ± 0.0.78	3.136 ± 0.191 ^{bc}	4.697 ± 0.191 ^{a}	2.476 ± 0.110 ^{cd}	3.424 ± 0.151 ^{b}	2.405 ± 0.177 ^{cd}	2.052 ± 0.072 ^{d}
Hydraulic conductivity (K_{sat})	cm h^{-1}	1.953 ± 0.073	1.643 ± 0. 082 ^{c}	2.392 ± 0.158 ^{b}	1.365 ± 0.094 ^{c}	3.475 ± 0.197 ^{a}	3.030 ± 0.499 ^{ab}	1.415 ± 0.038 ^{c}
Bulk density (*BD*)	g m^{-3}	1.085 ± 0.011	1.084 ± 0. 013 ^{b}	1.282 ± 0.078 ^{a}	1.123 ± 0.005 ^{ab}	0.912 ± 0.027 ^{c}	1.097 ± 0.028 ^{ab}	1.101 ± 0.011 ^{b}
Lake coverage	%	1.52 ± 0.3	1.58 ± 0.7 ^{bc}	7.93 ± 1.2 ^{a}	0.00 ± 0.0 ^{c}	2.95 ± 1.1 ^{b}	0.04 ± 0.0 ^{bc}	0.16 ± 0.1 ^{c}
Pond coverage	%	1.41 ± 0.2	1.45 ± 0.3 ^{b}	2.73 ± 0.3 ^{ab}	0.65 ± 0.1 ^{b}	0.57 ± 0.2 ^{b}	5.18 ± 2.5 ^{a}	1.30 ± 0.4 ^{b}
Alvar coverage	%	3.58 ± 0.5	9.80 ± 2.3 ^{a}	0.22 ± 0.2 ^{b}	0.74 ± 0.2 ^{b}	0.37 ± 0.2 ^{b}	0.00 ± 0.0 ^{b}	4.38 ± 0.6 ^{b}
Bog coverage	%	0.14 ± 0.0	0.01 ± 0.0 ^{b}	1.62 ± 0.2 ^{a}	0.00 ± 0.0 ^{b}	0.01 ± 0.0 ^{b}	0.00 ± 0.0 ^{b}	0.00 ± 0.0 ^{b}
Conifer swamp coverage	%	3.14 ± 0.3	8.08 ± 1.0 ^{a}	1.21 ± 0.3 ^{bc}	0.43 ± 0.2 ^{c}	3.65 ± 0.4 ^{b}	1.00 ± 0.5 ^{bc}	2.27 ± 0.3 ^{bc}
Deciduous swamp coverage	%	3.26 ± 0.3	3.83 ± 0.7 ^{a}	3.10 ± 0.7 ^{ab}	0.01 ± 0.0 ^{b}	4.49 ± 0.6 ^{a}	0.97 ± 0.5 ^{ab}	4.16 ± 0.7 ^{a}
Fen coverage	%	0.15 ± 0.0	0.43 ± 0.3 ^{a}	0.09 ± 0.0 ^{a}	0.01 ± 0.0 ^{a}	0.19 ± 0.1 ^{a}	0.00 ± 0.0 ^{a}	0.09 ± 0.0 ^{a}
Marsh coverage	%	2.25 ± 0.6	2.97 ± 1.2 ^{a}	0.08 ± 0.0 ^{a}	1.77 ± 0.6 ^{a}	0.71 ± 0.2 ^{a}	0.00 ± 0.0 ^{a}	3.64 ± 1.4 ^{a}
Deciduous coverage	%	17.59 ± 1.0	21.83 ± 2.2 ^{b}	41.24 ± 2.5 ^{a}	7.51 ± 1.3 ^{c}	17.61 ± 1.6 ^{b}	1.98 ± 0.8 ^{c}	16.22 ± 1.4 ^{b}
Conifer coverage	%	12.27 ± 0.9	21.82 ± 1.8 ^{b}	39.41 ± 2.2 ^{a}	1.18 ± 0.3 ^{e}	13.87 ± 0.9 ^{c}	0.65 ± 0.3 ^{de}	6.47 ± 0.7 ^{d}
Logging coverage	%	0.05 ± 0.0	0.00 ± 0.0 ^{b}	0.55 ± 0.2 ^{a}	0.00 ± 0.0 ^{b}	0.00 ± 0.0 ^{b}	0.00 ± 0.0 ^{b}	0.00 ± 0.0 ^{b}
Mine coverage	%	0.96 ± 0.3	1.90 ± 1.1 ^{ab}	4.08 ± 1.2 ^{a}	0.03 ± 0.0 ^{b}	0.11 ± 0.0 ^{b}	0.01 ± 0.0 ^{ab}	0.66 ± 0.3 ^{b}
Urban coverage	%	4.31 ± 1.1	0.10 ± 0.1 ^{b}	0.28 ± 0.1 ^{b}	0.25 ± 0.2 ^{b}	1.21 ± 0.5 ^{b}	73.56 ± 6.5 ^{a}	1.47 ± 0.5 ^{b}
Pasture coverage	%	17.64 ± 0.9	13.19 ± 1.3 ^{b}	2.68 ± 0.7 ^{c}	13.49 ± 1.3 ^{b}	16.06 ± 1.1 ^{b}	2.90 ± 0.8 ^{c}	28.08 ± 1.4 ^{a}
Cropland coverage	%	34.27 ± 1.6	15.83 ± 1.3 ^{d}	2.84 ± 1.0 ^{e}	74.57 ± 2.0 ^{a}	41.20 ± 1.6 ^{b}	18.62 ± 4.7 ^{d}	32.51 ± 1.7 ^{c}
Point source loading	tons P yr^{-1}	0.107±0.068	0.030±0.022 ^{b}	0.028±0.018 ^{b}	0.000±0.000 ^{b}	0.023±0.011 ^{b}	2.440±2.440 ^{a}	0.158±0.095 ^{b}
Net *TP* export	tons P yr^{-1}	3.095±0.447	1.080±0.206 ^{a}	2.840±0.507 ^{a}	2.218±1.632 ^{a}	4.038±0.957 ^{a}	3.729±2.300 ^{a}	2.873±0.584 ^{a}
TP Yield	tons P km^{-2} yr^{-1}	0.063±0.017	0.021±0.012 ^{bc}	0.008±0.002 ^{c}	0.528±0.253 ^{a}	0.040±0.008 ^{bc}	0.209±0.141 ^{abc}	0.170±0.092 ^{b}
TP concentration	mg P L^{-1}	0.029±0.004	0.017±0.001 ^{b}	0.014±0.001 ^{b}	0.103±0.073 ^{a}	0.027±0.002 ^{b}	0.018±0.002 ^{ab}	0.069±0.023 ^{a}

(209 kg P km^{-2} yr^{-1}). Winter and Duthie (2000) provided an estimate of ≈500 kg P km^{-2} yr^{-1} of areal phosphorus export (i.e., yield) from urban areas of Laurel Creek, located in Southern Ontario. Dietz and Clausen (2008) reported that TP loading was highly correlated with total impervious area, as extensive paving increases soil imperviousness and reduces storage capacity, thereby generating fast runoff (Hatt et al., 2004). Our DLM analysis aligns with these findings in that the relatively urbanized catchments near the Bay of Quinte show more dynamic flow patterns with significant within-year and year-to-year variability as well as tighter relationship with the local precipitation.

Consistent with the popular notion in the literature, agricultural activities appear to primarily shape the non-point TP export from the Bay of Quinte watershed. Excessive fertilizer or manure application in croplands, management practices (e.g., crop types and tillage methods), and soil hydrological characteristics (e.g., hydraulic conductivity and permeability) generally determine soil phosphorus level and consequent losses through runoff from agricultural sites (Pote et al., 1996; Sims et al., 2000). SOM identified two clusters characterized by high areal cropland coverages. Cluster 3 had the highest *TP* yield and concentration, while Cluster 4 had the largest net TP export. The former cluster comprises the township areas of Prince Edward County and Lennox–Addington. In Prince Edward County, corn and alfalfa occupied the largest fraction of cropland areas (37% of corn, ≈36% of alfalfa, and 25% of wheat), while >50% of the same locations did not implement tillage methods, such as surface or injected soil tillage. By contrast, in Lennox–Addington, alfalfa accounted for 57% of cropland followed by corn (31%) and wheat (12%), while tillage methods were more frequently applied (>60%; Quinte Conservation, personal communication). Cluster 4 encompasses the township areas within Kawartha Lakes and Northumberland County. The Kawartha Lakes area has a higher proportion of alfalfa (55%), followed by corn (24%) and wheat (18%), whereas the Northumberland County area has the largest proportion of untilled cropland (≈57% of no tillage, ≈29% of surface soil tillage, and ≈13% of injected soil tillage). Moreover, Cluster 4 is characterized by the highest hydraulic conductivity among all clusters delineated, which may explain the lower TP yield and concentrations relative to Cluster 3. That is, the soil's high hydraulic conductivity could attenuate phosphorus land-to-stream delivery (Weld et al., 2001), which in turn moderates phosphorus export from the corresponding sites.

Other dominant land uses in the Bay of Quinte watershed include forested and pasture areas. Consistent with earlier reports (Dillon and Kirchner, 1975), the forested locations had the lowest TP yield (≈8 kg P km^{-2} yr^{-1}) and concentration (≈14 μg P L^{-1}) (Table 1), as there are no major anthropogenic sources of TP loading and the runoff ratio (the percentage of rainfall volume to runoff) is typically very low (Corbett et al., 1997). Counter to urban sites, forested areas have larger capacity to store surface runoff (Corbett et al., 1997; Harris, 2001). Regarding the pasture land, earlier work by Beaulac and Reckhow (1982) stated that pasture and grazed areas are comparable to agricultural areas with respect to their potential impact as non-point sources. Likewise, Nash and Halliwell (2000) noted that substantial variability characterizes the fate and transport of phosphorus in pasture-based grazing systems. Nash et al. (2000) further showed that phosphorus mobilization in pasture-dominated watersheds occurs primarily as a result of dissolution, rather than erosional processes. In North Carolina, Butler et al. (2006) estimated 70 ~ 350 kg P km^{-2} yr^{-1} of TP yield derived from riparian pasture, and also found that dissolved phosphorus export increased significantly as pasture coverage expanded with heavy rainfall. In the Bay of Quinte watershed, the pasture-dominated cluster (#6) exported approximately 170 kg P km^{-2} yr^{-1}, but since the same areas are also characterized by agricultural activities (32.5% of land use), it is difficult to unequivocally estimate the impact of pasture. On a final note, wetlands are well known as nutrient sinks, playing a key role in phosphorus removal, and Winter et al. (2002) showed a TP export decrease that is inversely related to wetland areal coverage. However, Dillon and Molot (1997) showed a TP export increase proportional to wetland areal coverage in south-central Ontario, and Paterson et al. (2006) demonstrated a similarly strong positive relationship in twenty watersheds of this region. Thus, the positive relationship between net TP loads and wetland area found in our study could be a plausible result. Furthermore, Cluster 1 included the three most dominant wetlands (alvar, coniferous swamp, and fen), but the corresponding fractional areas are fairly small to infer about their relative contribution to the TP loads collectively exported from these areas (Table 2).

To recap, we were able to discern distinct land use patterns and morphological characteristics in relation to TP export in the Bay of Quinte watershed. Self-organizing map analysis delineated six spatial clusters in the Bay of Quinte watershed, representing one forested, two agricultural, one urban, one pasture-dominated, and one transitional area. Our study showed that agricultural and urban land areas primarily regulate riverine TP dynamics. Tributaries draining agricultural catchments exhibit considerable variability, depending on management practices and soil properties. In particular, the hydraulic conductivity of the soils could significantly modulate phosphorus land-to-stream delivery, and therefore determine phosphorus export from agricultural areas. Urbanized catchments near the Bay of Quinte show more dynamic flow patterns with significant within- and among-year variability and stronger relationship with precipitation. This "flashy" behavior of urban sites is accompanied by a relatively high net TP export and TP yield. Pasture-based grazing systems similarly appear to play a major role in determining the fate and transport of phosphorus in the area. Our delineation of the spatial TP loading patterns will be essential in guiding an on-going watershed modeling exercise that aims to quantify nutrient export coefficients and delivery rates from different subcatchments and thus verifying our key findings regarding the nutrient export "hot spots" and the potential effects of climate change on the severity of eutrophication problems in the Bay of Quinte.

Acknowledgment

This project was undertaken with the financial support of the Lower Trent Region Conservation Authority provided through the Bay of Quinte Remedial Action Plan Restoration Council. Aspects of the project were also supported by the Natural Sciences and Engineering Research Council of Canada (Discovery Grant awarded to George Arhonditsis).

Appendix A. Supplementary data

Supplementary data to this article can be found online at http://dx.doi.org/10.1016/j.jglr.2016.07.008.

References

Arhonditsis, G.B., Kim, D.-K., Shimoda, Y., Zhang, W., Watson, S., Mugalingam, S., Dittrich, M., Geater, K., McClure, C., Keene, B., Morley, A., Richards, A., Long, T., Rao, Y.R., Kalinauskas, R., 2016. Integration of best management practices in the Bay of Quinte watershed with the phosphorus dynamics in the receiving water body: what do the models predict? Aquat. Ecosyst. Health Manag. 19, 1–18.

Bailey, R.C., Grapentine, L., Stewart, T.J., Schaner, T., Chase, M.E., Mitchell, J.S., Coulas, R.A., 1999. Dreissenidae in Lake Ontario: impact assessment at the whole lake and Bay of Quinte spatial scales. J. Great Lakes Res. 25, 482–491.

Bay of Quinte Remedial Action Plan (BQRAP), 1987. Bay of Quinte Remedial Action Plan.

Beaulac, M.N., Reckhow, K.H., 1982. An examination of land use–nutrient export relationships. J. Am. Water Resour. Assoc. 18, 1013–1024.

Butcher, J.B., 2003. Buildup, washoff, and event mean concentrations. J. Am. Water Resour. Assoc. 39, 1521–1528.

Butler, D.M., Franklin, D.H., Ranells, N.N., Poore, M.H., Green, J.T., 2006. Ground cover impacts on sediment and phosphorus export from manured riparian pasture. J. Environ. Qual. 35, 2178–2185.

Chon, T.-S., Park, Y.-S., Moon, K.H., Cha, E.Y., 1996. Patterning communities by using an artificial neural network. Ecol. Model. 90, 69–78.

Corbett, C.W., Wahl, M., Porter, D.E., Edwards, D., Moise, C., 1997. Nonpoint source runoff modeling: a comparison of a forested watershed and an urban watershed on the South Carolina coast. J. Exp. Mar. Biol. Ecol. 213, 133–149.

Dermott, R., Bonnell, R., 2011. Benthic Fauna in the Bay of Quinte. Bay of Quinte Remedial Action Plan: Mornitoring Report #20, Kingston, Ontario, Canada, pp. 51–71.
Dermott, R., Bonnell, R., Carou, S., Dow, J., Jarvis, P., 2003. Spatial Distribution and Population Structure of the Mussels *Dreissena polymorpha* and *Dreissena bugensis* in the Bay of Quinte, Lake Ontario, 1998 and 2000. Burlington, Ontario L7R 4 A6.
Dietz, M.E., Clausen, J.C., 2008. Stormwater runoff and export changes with development in a traditional and low impact subdivision. J. Environ. Manag. 87, 560–566.
Dillon, P.J., Kirchner, W.B., 1975. The effects of geology and land use on the export of phosphorus from watersheds. Water Res. 9, 135–148.
Dillon, P.J., Molot, L.A., 1997. Effect of landscape form on export of dissolved organic carbon, iron, and phosphorus from forested stream catchments. Water Resour. Res. 33, 2591–2600.
Djodjic, F., Börling, K., Bergström, L., 2004. Phosphorus leaching in relation to soil type and soil phosphorus content. J. Environ. Qual. 33, 678–684.
Duan, S., Kaushal, S.S., Groffman, P.M., Band, L.E., Belt, K.T., 2012. Phosphorus export across an urban to rural gradient in the Chesapeake Bay watershed. J. Geophys. Res. Biogeosci. 117, G01025.
ESRI, 2004. ArcGIS Desktop: Release 9.3. Environmental Systems Research Institute, Redlands, CA.
Giraudel, J.L., Lek, S., 2001. A comparison of self-organizing map algorithm and some conventional statistical methods for ecological community ordination. Ecol. Model. 146, 329–339.
Ha, J.-Y., Hanazato, T., Chang, K.-H., Jeong, K.-S., Kim, D.-K., 2015. Assessment of the lake biomanipulation by introducing both piscivorous rainbow trout and herbivorous daphnids using self-organizing map analysis: a case study in Lake Shirakaba, Japan. Ecol. Inform. 29, 182–191.
Harris, G.P., 2001. Biogeochemistry of nitrogen and phosphorus in Australian catchments, rivers and estuaries: effects of land use and flow regulation and comparisons with global patterns. Mar. Freshw. Res. 52, 139–149.
Hatt, B.E., Fletcher, T.D., Walsh, C.J., Taylor, S.L., 2004. The influence of urban density and drainage infrastructure on the concentrations and loads of pollutants in small streams. Environ. Manag. 34, 112–124.
Kim, D.-K., Zhang, W., Rao, Y., Watson, S., Mugalingam, S., Labencki, T., Dittrich, M., Morley, A., Arhonditsis, G.B., 2013. Improving the representation of internal nutrient recycling with phosphorus mass balance models: a case study in the Bay of Quinte, Ontario, Canada. Ecol. Model. 256, 53–68.
Kinstler, P., Morley, A., 2011. Point source phosphorus loadings 1965 to 2009. Bay of Quinte Remedial Action Plan: Monitoring Report #20, Kingston, Ontario, Canada, pp. 15–17.
Kohonen, T., 1982. Self-organized formation of topologically correct feature maps. Biol. Cybern. 43, 59–69.
Kohonen, T., 1997. Self-Organizing Maps. Springer, New York (426 pp.).
Lamon, E.C., Carpenter, S.R., Stow, C.A., 1998. Forecasting PCB concentrations in Lake Michigan salmonids: a dynamic linear model approach. Ecol. Appl. 8, 659–668.
Leisti, K.E., Millard, E.S., Minns, C.K., 2006. Assessment of Submergent Macrophytes in the Bay of Quinte, Lake Ontario, August 2004, Including Historical Context. Dept. of Fisheris and Oceans Canada.
Long, T., Wellen, C., Arhonditsis, G., Boyd, D., 2014. Evaluation of stormwater and snow-melt inputs, land use and seasonality on nutrient dynamics in the watersheds of Hamilton Harbour, Ontario, Canada. J. Great Lakes Res. 40, 964–979.
Long, T., Wellen, C., Arhonditsis, G., Boyd, D., Mohamed, M., O'Connor, K., 2015. Estimation of tributary total phosphorus loads to Hamilton Harbour, Ontario, Canada, using a series of regression equations. J. Great Lakes Res. 41, 780–793.
Mahmood, M., Bhavsar, S.P., Arhonditsis, G.B., 2013. Examination of temporal DDT trends in Lake Erie fish communities using dynamic linear modeling. J. Great Lakes Res. 39, 437–448.
McGlynn, B.L., McDonnell, J.J., Seibert, J., Kendall, C., 2004. Scale effects on headwater catchment runoff timing, flow sources, and groundwater-streamflow relations. Water Resour. Res. 40, W07504.
Minns, C.K., Hurley, D.A., Nicholls, K.H., 1986a. Project Quinte: Point-Source Phosphorus Control and Ecosystem Response in the Bay of Quinte, Lake Ontario. Dept. of Fisheries and Oceans, Ottawa.
Minns, C.K., Owen, G.E., Johnson, M.G., 1986b. Nutrient loads and budgets in the Bay of Quinte, Lake Ontario, 1965–81. In: Minns, C.K., Hurley, D.A., Nicholls, K.H. (Eds.), Project Quinte: Point-Source Phosphorus Control and Ecosystem Response in the Bay of Quinte, Lake Ontario. Canadian Special Publication of Fisheries and Aquatic Sciences, Ottawa, pp. 59–76.
Minns, C.K., Moore, J.E., Seifried, K.E., 2004. Nutrient Loads and Budgets in the Bay of Quinte, Lake Ontario, 1972 to 2001. Burlington, Ontario.
Moatar, F., Meybeck, M., 2005. Compared performances of different algorithms for estimating annual nutrient loads discharged by the eutrophic River Loire. Hydrol. Process. 19, 429–444.
Moore, R.B., Johnson, C.M., Robinson, K.W., Deacon, J.R., 2004. Estimation of Total Nitrogen and Phosphorus in New England Streams Using spatially Referenced Regression Models. New Hampshire.
Nash, D.M., Halliwell, D.J., 2000. Tracing phosphorous transferred from grazing land to water. Water Res. 34, 1975–1985.
Nash, D., Hannah, M., Halliwell, D., Murdoch, C., 2000. Factors affecting phosphorus export from a pasture-based grazing system. J. Environ. Qual. 29, 1160–1166.
Park, Y.-S., Kwon, Y.-S., Hwang, S.-J., Park, S., 2014. Characterizing effects of landscape and morphometric factors on water quality of reservoirs using a self-organizing map. Environ. Model. Softw. 55, 214–221.
Paterson, A.M., Dillon, P.J., Hutchinson, N.J., Futter, M.N., Clark, B.J., Mills, R.B., Reid, R.A., Scheider, W.A., 2006. A review of the components, coefficients and technical assumptions of Ontario's Lakeshore Capacity Model. Lake Reservoir Manage. 22, 7–18.
Pfeifer, L.R., Bennett, E.M., 2011. Environmental and social predictors of phosphorus in urban streams on the Island of Montreal, Quebec. Urban Ecosyst. 14, 485–499.
Pole, A., West, M., Harrison, J., 1994. Applied Bayesian Forecasting and Time Series Analysis. Champman & Hall/CRC, Washington, D.C. (409 pp.).
Pote, D.H., Daniel, T.C., Moore, P.A., Nichols, D.J., Sharpley, A.N., Edwards, D.R., 1996. Relating extractable soil phosphorus to phosphorus losses in runoff. Soil Sci. Soc. Am. J. 60, 855–859.
Preston, S.D., Bierman, V.J., Silliman, S.E., 1989. An evaluation of methods for the estimation of tributary mass loads. Water Resour. Res. 25, 1379–1389.
Rode, M., Arhonditsis, G., Balin, D., Kebede, T., Krysanova, V., van Griensven, A., van der Zee, S.E.A.T.M., 2010. New challenges in integrated water quality modelling. Hydrol. Process. 24, 3447–3461.
Shimoda, Y., Watson, S., Palmer, M.E., Koops, M., Mugalingam, S., Morley, A., Arhonditsis, G.B., 2016. Delineation of the role of nutrient variability and dreissenids (Mollusca, Bivalvia) on phytoplankton dynamics in the Bay of Quinte, Ontario, Canada. Harmful Algae 55, 121–136.
Sims, J.T., Edwards, A.C., Schoumans, O.F., Simard, R.R., 2000. Integrating soil phosphorus testing into environmentally based agricultural management practices. J. Environ. Qual. 29, 60–71.
Soldat, D.J., Petrovic, A.M., 2008. The fate and transport of phosphorus in turfgrass ecosystems. Crop Sci. 48, 2051–2065.
Soldat, D., Petrovic, A.M., Ketterings, Q., 2009. Effect of soil phosphorus levels on phosphorus runoff concentrations from turfgrass. Water Air Soil Pollut. 199, 33–44.
Stow, C.A., Lamon, E.C., Qian, S.S., Schrank, C.S., 2004. Will Lake Michigan lake trout meet the Great Lakes strategy 2002 PCB reduction goal? Environ. Sci. Technol. 38, 359–363.
Taraborelli, A.C., Fox, M.G., Johnson, T.B., Schaner, T., 2010. Round goby (*Neogobius melanostomus*) population structure, biomass, prey consumption and mortality from predation in the Bay of Quinte, Lake Ontario. J. Great Lakes Res. 36, 625–632.
United States Environmental Protection Agency, 1978. Great Lakes water quality agreement. http://www.epa.gov/greatlakes/glwqa/.
van Es, H.M., Schindelbeck, R.R., Jokela, W.E., 2004. Effect of manure application timing, crop, and soil type on phosphorus leaching. J. Environ. Qual. 33, 1070–1080.
Vesanto, J., Alhoniemi, E., 2000. Clustering of the self-organizing map. IEEE Trans. Neural Netw. 11, 586–600.
Vesanto, J., Himberg, J., Alhoniemi, E., Parhankangas, J., 2000. SOM Toolbox for Matlab 5.
Weld, J., Sharpley, A., Beegle, D., Gburek, W., 2001. Identifying critical sources of phosphorus export from agricultural watersheds. Nutr. Cycl. Agroecosyst. 59, 29–38.
Wellen, C., Arhonditsis, G.B., Long, T., Boyd, D., 2014. Accommodating environmental thresholds and extreme events in hydrological models: a Bayesian approach. J. Great Lakes Res. 40, 102–116.
White, M.D., Greer, K.A., 2006. The effects of watershed urbanization on the stream hydrology and riparian vegetation of Los Peñasquitos Creek, California. Landsc. Urban Plan. 74, 125–138.
Winter, J.G., Duthie, H.C., 2000. Export coefficient modeling to assess phosphorus loading in an urban watershed. J. Am. Water Resour. Assoc. 36, 1053–1061.
Winter, J.G., Dillon, P.J., Futter, M.N., Nicholls, K.H., Scheider, W.A., Scott, L.D., 2002. Total phosphorus budgets and nitrogen loads: Lake Simcoe, Ontario (1990 to 1998). J. Great Lakes Res. 28, 301–314.
Withers, P.J.A., Jarvie, H.P., 2008. Delivery and cycling of phosphorus in rivers: a review. Sci. Total Environ. 400, 379–395.

Glossary

Best matching unit (BMU): Virtual units compete with each other for having a minimum distance towards the selected sampling neuron. BMU refers to one of the virtual units having the minimum distance at the end of data learning. It is often called “winning neuron”.
Global ordering: Data ordination generated by continuous local relaxation during the learning process on the entire map.
Input layer: Layer of neural cells projected on two-dimensional grid that receives input variables directly.
Local relaxation or smoothing effect: During the learning process, the nonlinear projection is formed. The neural nodes are getting topologically close in the array up to a certain geometric distance, which will activate each other to learn something from the same input vector. This results in a local relaxation on the weight vectors of neurons in the neighborhood.
Neighborhood function: During the learning process, the BMU is defined. All the neighboring neurons around the BMU are updated using the neighborhood function.
Output layer: The hexagonal layer where all neurons occupy specific locations after the learning process.
Weight vector: Virtual parametric vectors that activate input vectors for data learning. These vectors are initialized randomly, and gradually updated during the learning process.

ELECTRONIC SUPPLEMENTARY MATERIAL (ESM)

EVALUATING THE RELATIONSHIPS BETWEEN WATERSHED PHYSIOGRAPHY, LAND USE PATTERNS, AND PHOSPHORUS LOADING IN THE BAY OF QUINTE BASIN, ONTARIO, CANADA

Dong-Kyun Kim[1], Samarth Kaluskar[1], Shan Mugalingam[2], George B. Arhonditsis[1*]

[1]Ecological Modelling Laboratory,
Department of Physical & Environmental Sciences, University of Toronto,
Toronto, Ontario, Canada, M1C1A4

[2]Lower Trent Conservation,
Trenton, Ontario, Canada, K8V 5P4

* Corresponding author
E-mail: georgea@utsc.utoronto.ca, Tel.: +1 416 208 4858; Fax: +1 416 287 7279.

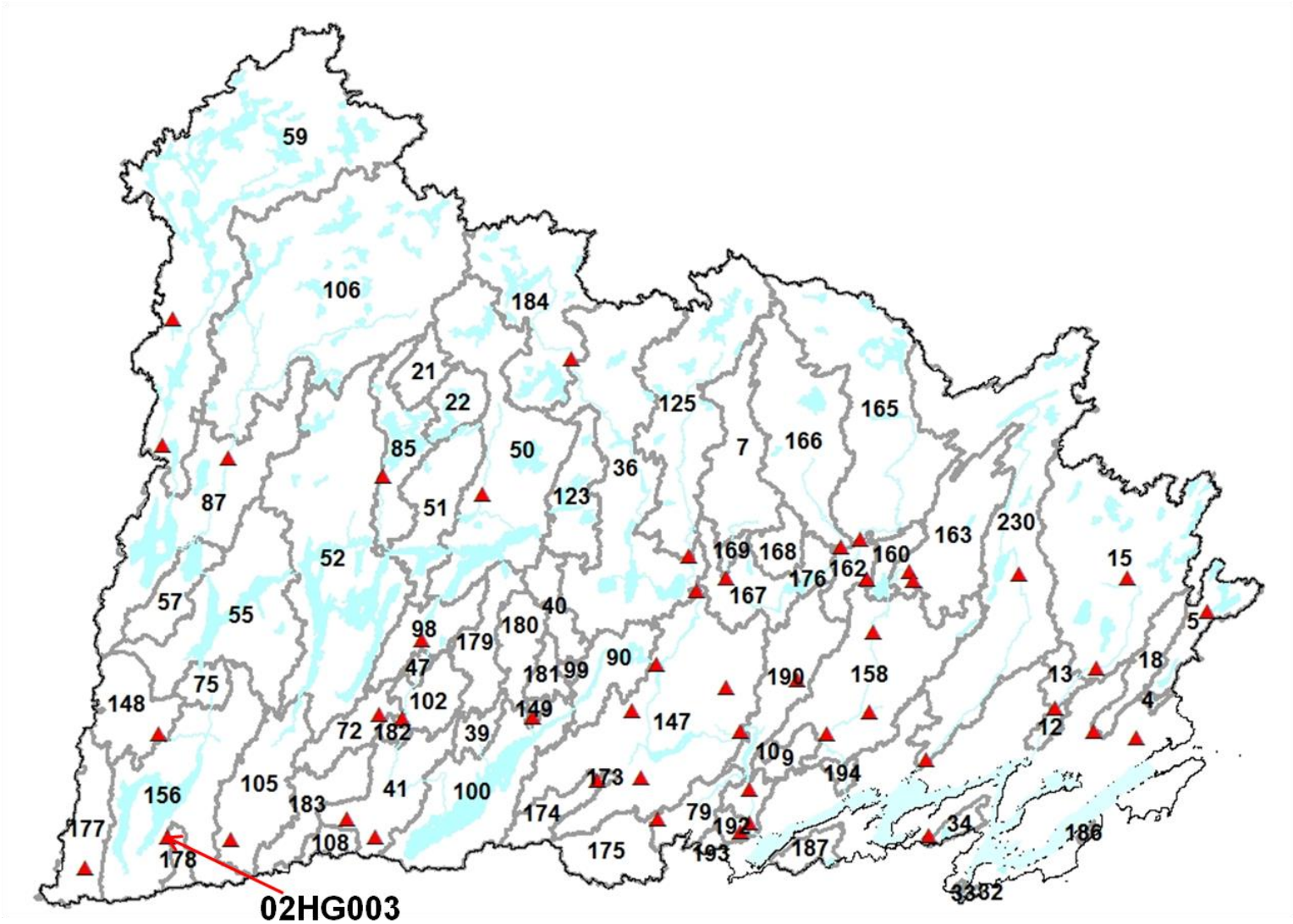

Figure S1: 73 gauged subwatersheds and 48 flow monitoring stations in the Bay of Quinte watershed. The numbers indicate the subwatershed IDs.

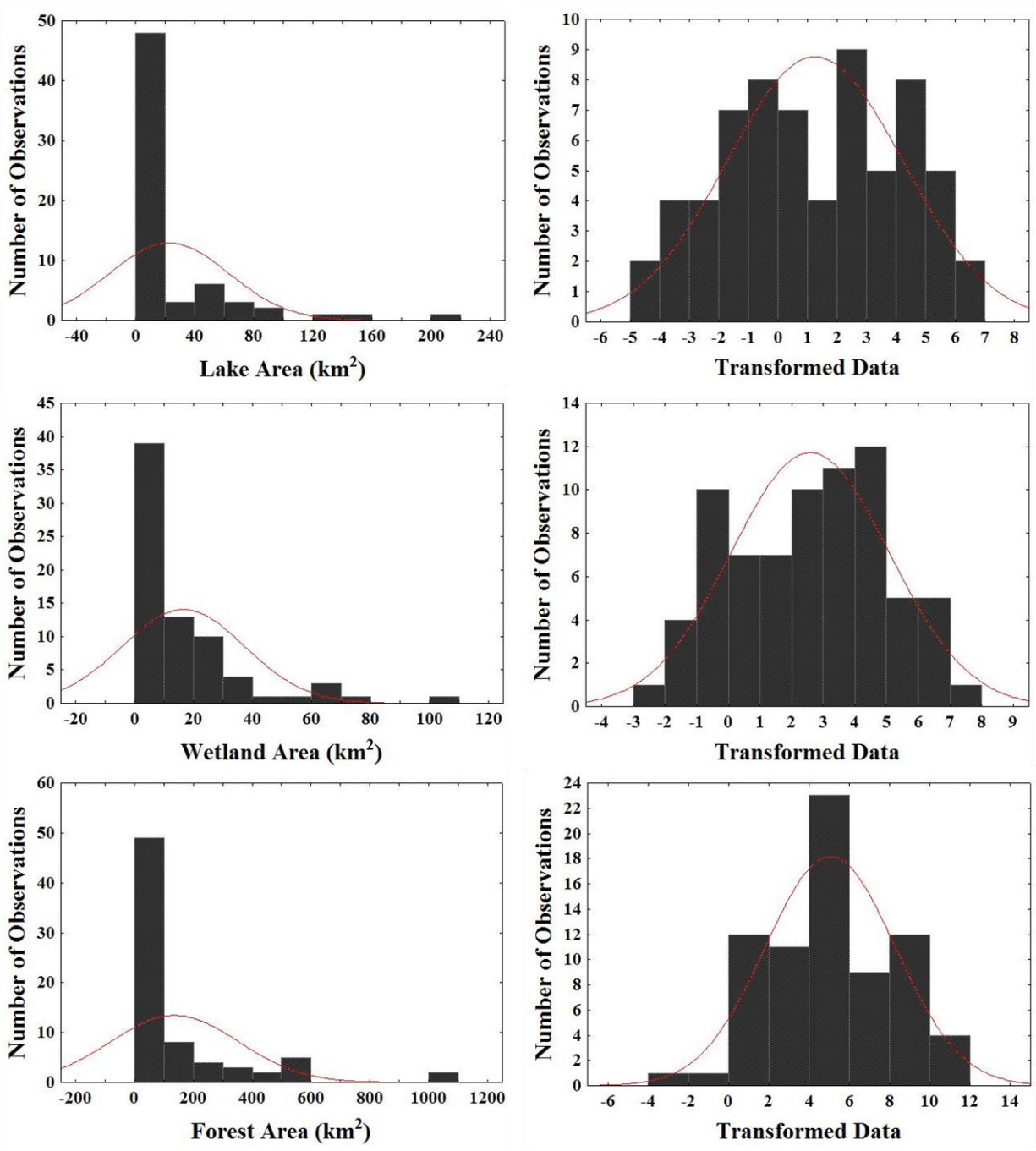

Figure S2: Frequency distribution of land-use sizes in the Bay of Quinte watershed (*N*=73). The left panels depict observation frequency in normal scale, and the right panels represent the empirical distribution after the Box-Cox transformation.

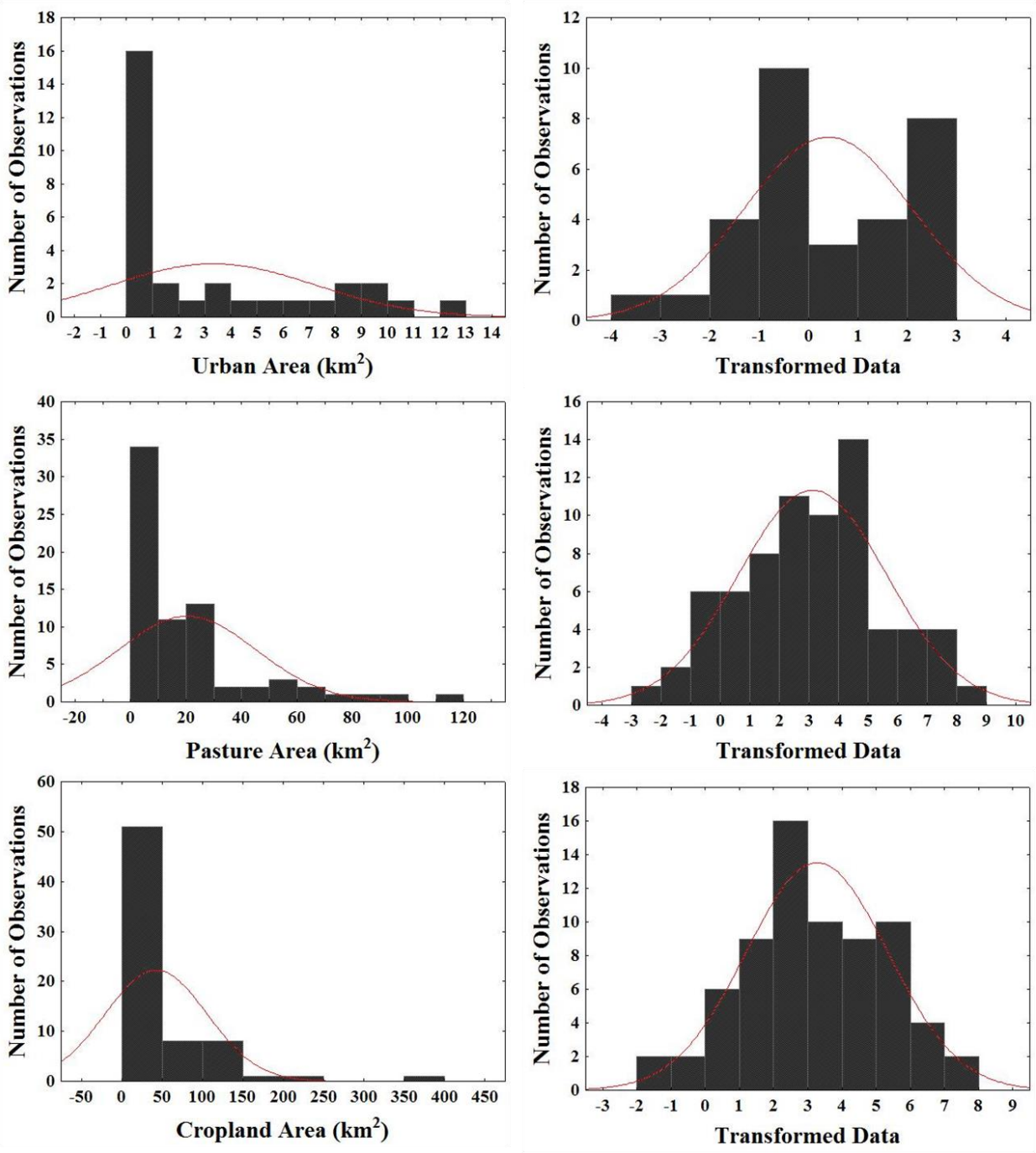

Figure S2 (continued)

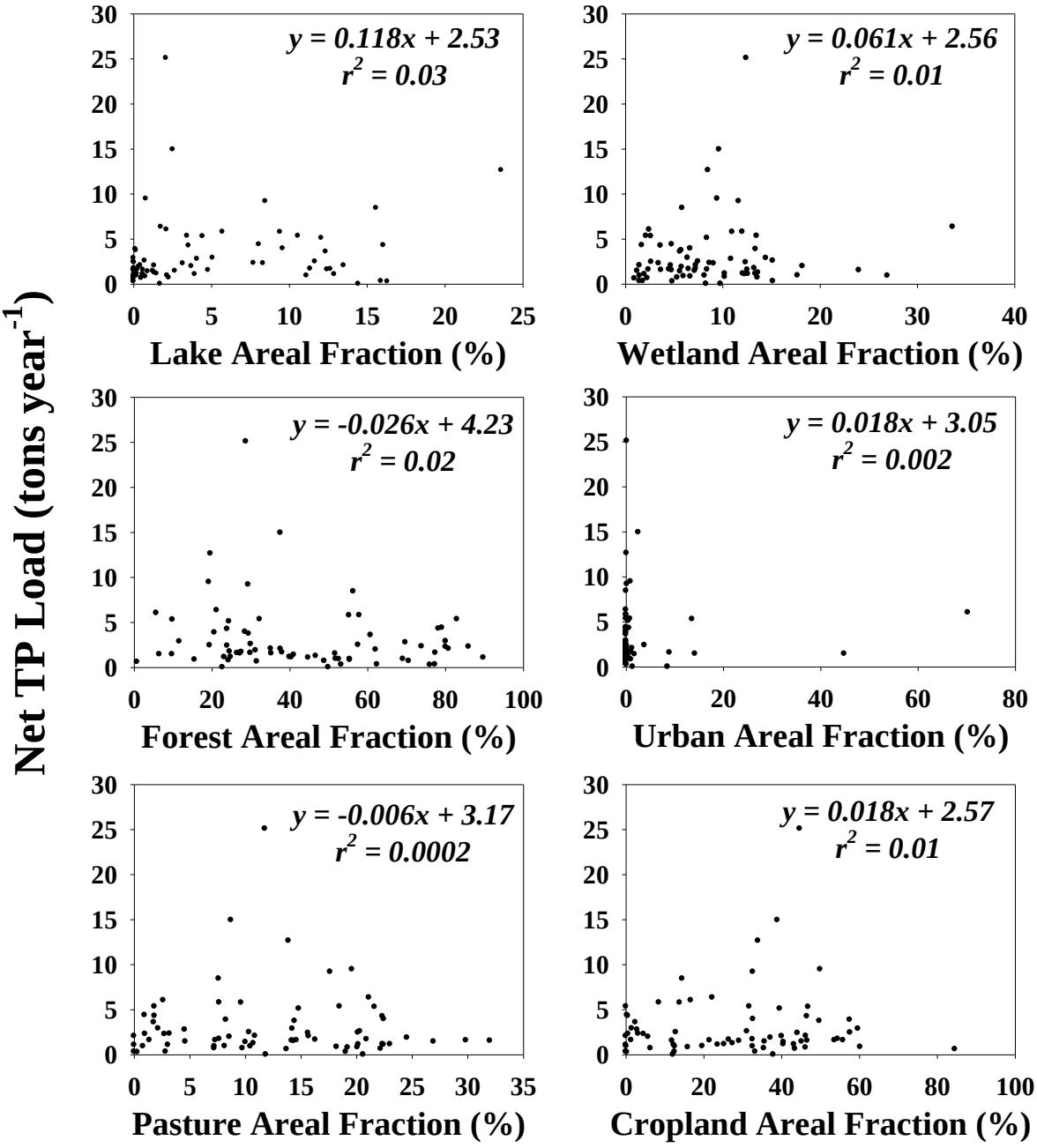

Figure S3: Relationships between annual net TP exports and different land-use areal fractions (lake, wetland, forest, urban land, pasture and cropland) in the 73 gauged subwatersheds.

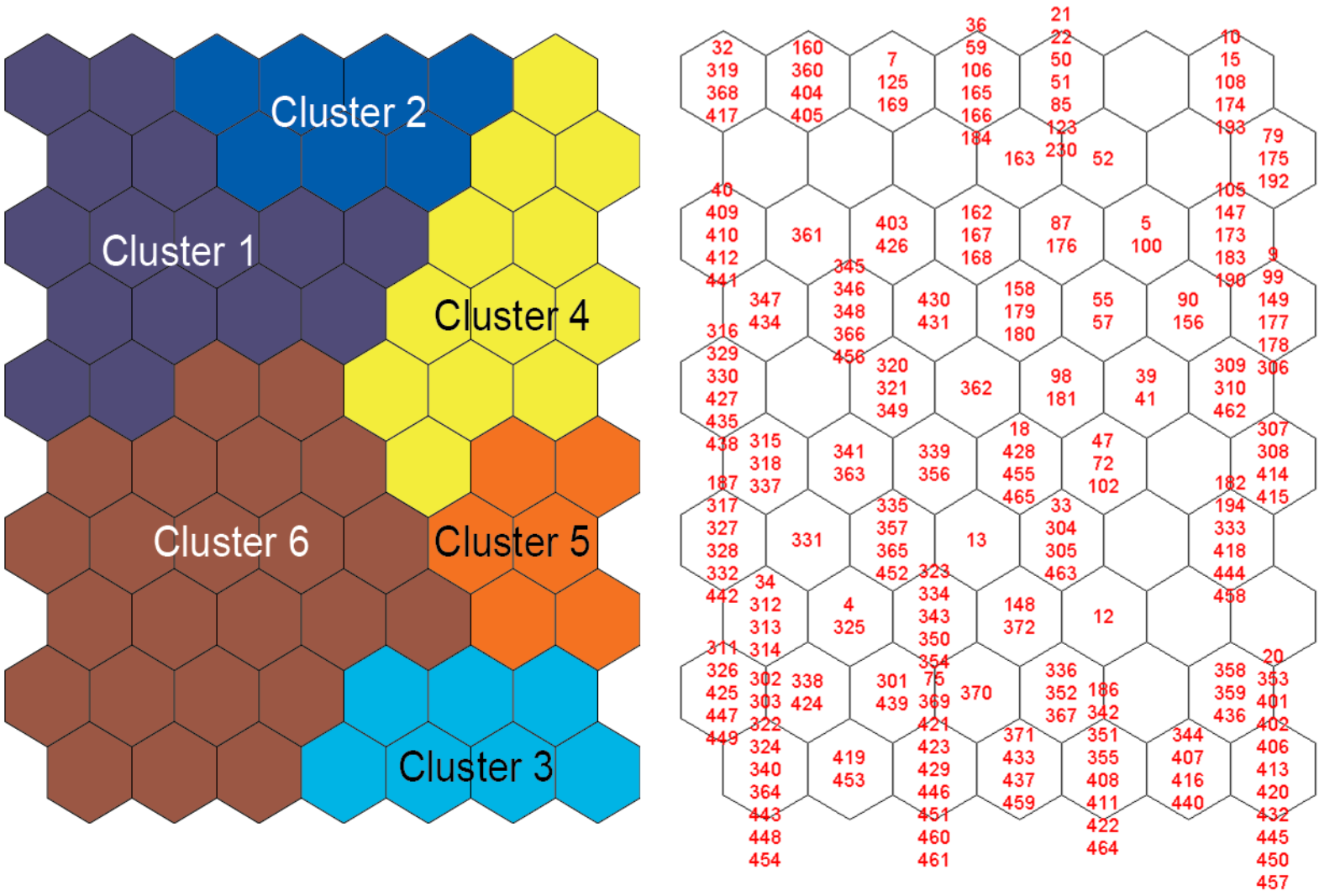

Figure S4: Data clustering by SOM. Numbers lower than 300 indicate 73 gauged subwatershed IDs represented in Table S2. Subwatersheds in which the ID numbers are greater than 300 refer to 137 ungauged subwatershed IDs.

Table S1: Catchment size and mean flow rates based on 48 monitoring stations in the Bay of Quinte watershed.

Station ID	Latitude	Longitude	N of years	Watershed	Catchment (km^2)	Mean ($m^3 s^{-1}$)	CV (%)
02HF002	44.73	-78.82	48	Trent River	1281.6	19.6	21.6
02HF003	44.71	-78.68	48	Trent River	1251.9	18.5	22.4
02HF004	44.93	-78.79	16	Trent River	18.3	0.2	20.8
02HG001	44.29	-78.84	23	Trent River	184.9	1.7	25.0
02HG002	44.09	-79.01	18	Trent River	41.7	0.3	29.7
02HG003	44.13	-78.83	3	Trent River	33.9	0.3	52.8
02HH001	44.64	-78.14	25	Trent River	254.2	3.6	20.8
02HH002	44.68	-78.35	21	Trent River	306.5	4.4	19.5
02HH003	44.12	-78.70	6	Trent River	30.4	0.3	18.4
02HJ001	44.30	-78.32	48	Trent River	115.8	1.1	27.5
02HJ002	44.42	-78.28	28	Trent River	7336.4	85.1	20.4
02HJ003	44.30	-78.04	34	Trent River	282.7	2.9	24.3
02HJ005	44.12	-78.39	7	Trent River	10.4	0.1	15.7
02HJ006	44.31	-78.37	4	Trent River	106.7	1.2	50.2
02HJ007	44.15	-78.45	4	Trent River	45.5	0.6	15.3
02HK002	44.37	-77.77	54	Trent River	9146.3	94.4	25.5
02HK003	44.48	-77.68	51	Trent River	1930	23.7	24.8
02HK004	44.26	-77.60	31	Trent River	12005.4	143.2	24.1
02HK005	44.84	-77.93	34	Trent River	440.5	6.5	19.5
02HK006	44.54	-77.70	32	Trent River	551.8	7.4	20.3
02HK007	44.13	-77.79	28	Trent River	161.9	2.0	16.8
02HK008	44.34	-77.48	17	Trent River	92.9	1.1	20.5
02HK009	44.20	-77.91	21	Trent River	83.2	0.9	18.2
02HK010	44.12	-77.59	4	Trent River	12532.2	125.2	15.3
02HK011	44.11	-77.61	17	Trent River	33.1	0.4	27.4
02HK014	44.17	-77.59	1	Trent River	12499	166.7	N/A
02HK015	44.20	-77.82	3	Trent River	78.8	1.1	31.2
02HK016	44.30	-77.83	4	Trent River	33	0.4	35.2
02HK017	44.33	-77.63	3	Trent River	111.9	1.3	46.3
02HL001	44.25	-77.42	95	Moira River	2602.9	30.5	25.8
02HL003	44.54	-77.37	55	Moira River	430	5.2	24.8
02HL004	44.55	-77.33	53	Moira River	679.4	8.4	23.4
02HL005	44.50	-77.62	45	Moira River	297.8	3.8	22.1
02HL007	44.49	-77.32	8	Moira River	1767.7	21.1	25.7
02HL008	44.50	-77.23	4	Moira River	306.3	4.1	33.0
02HL101	44.49	-77.32	4	Moira River	1767.7	25.1	13.0
02HL102	44.48	-77.22	6	Moira River	172.4	2.8	27.1
02HL103	44.28	-77.33	14	Moira River	207.8	3.1	25.0
02HL104	44.41	-77.31	1	Moira River	2198.1	25.3	N/A
02HM001	44.28	-76.93	39	Napanee River	778.5	9.2	29.0
02HM002	44.47	-76.76	54	Napanee River	178.4	2.0	21.1
02HM007	44.33	-76.84	37	Napanee River	699.5	8.8	19.9
02HM003	44.21	-77.21	52	Salmon River	906.7	10.8	24.4
02HM010	44.49	-76.99	7	Salmon River	533.6	7.1	20.8

Station ID	Latitude	Longitude	N of years	Watershed	Catchment (km^2)	Mean ($m^3 s^{-1}$)	CV (%)
02HE003	44.09	-77.21	7	Demorestville Creek	32.9	0.4	9.9
02HM004	44.24	-76.85	45	Wilton Creek	104.4	1.5	22.8
02HM006	44.23	-76.76	40	Millhaven Creek	144.2	2.0	22.2
02HM011	44.41	-76.59	4	Millhaven Creek	57.7	0.7	39.4

Table S2: Areal extent of different land-use based on 73 gauged subwatersheds in the Bay of Quinte watershed

Station ID	ID	Unit	Lake	Crop land	Urban land	Conifer forest	Deciduous forest	Pasture	Alvar	Bog	Fen	Swamp	Marsh	Logging	Mining
06018000402	4		0.06	2.19	0.91	0.51	2.18	3.03	0.93		0.03	0.25	0.07		
06018000502	5		15.55	32.54		7.89	38.90	20.03	2.26		0.99	3.22	1.54		
17002601902	7		8.78	12.76		113.76	108.01	7.59		1.18		23.97		0.86	
17002602102	9		0.01	28.22		5.50	7.23	3.97			0.07	5.97	0.84		
17002602202	10			2.54		1.21	3.56	0.22				0.11			
17003500102	12		1.15	12.18	3.53	0.54	2.02	5.62	0.57			0.05	0.06		0.25
17003500202	13		0.36	15.66		3.21	11.88	10.22	5.79		0.06	1.77			1.33
17003500402	15		68.59	100.92		96.21	306.29	70.14	10.15	3.27	7.85	49.15	9.60		6.04
17003700302	18		0.33	38.82		10.59	22.06	25.64	4.81		0.16	0.99	0.10		0.93
17000900102	20			1.80		0.02		0.29				0.02			
17002113802	21		3.13			34.28	37.09	0.01		1.57					3.43
17002113902	22		14.46			41.32	29.03			1.64				0.05	4.50
17000800102	32			0.25		0.44	0.64	0.39	0.20			0.10			
17000800202	33			1.93		0.10	0.28	0.46	0.13			0.33			
17001400102	34	km^2	1.58	3.91		1.38	7.60	10.53	2.91		0.05	4.72	0.22		
17002100302	36		58.60	24.28	1.57	261.50	300.22	24.33		8.31	1.52	56.06		13.95	9.72
17002100602	39		0.11	21.00		6.73	6.16	11.60				6.27			
17002100702	40		0.18	11.71		27.08	21.78	6.72			2.85	22.15			0.33
17002100802	41		1.84	115.64	2.21	16.52	28.05	45.37				21.88			0.01
17002101302	47		0.64	8.48		1.91	2.45	4.07				0.66			
17002101602	50		80.83	9.06	6.98	274.79	228.48	9.03		12.60	0.71	15.98		1.79	9.60
17002101702	51		28.39	5.65		71.42	68.37	4.09		2.62		10.34			39.06
17002101802	52		141.82	131.98	0.42	281.14	231.80	69.33		13.77	0.73	33.87	4.95		0.41
17002102102	55		49.14	167.70		88.57	57.83	115.22			1.63	29.18	3.46		
17002102302	57		14.31	41.05		19.72	15.08	26.36				8.62	0.52		0.40
17002102502	59		216.86	7.19	8.81	358.37	699.13	25.01		18.53	1.12	3.44	0.08	9.71	3.24
17002103802	72		0.04	51.12	4.43	11.96	15.83	18.15			0.71	13.65			0.07
17002104102	75		1.54	26.06	8.18	0.91	4.74	15.53				0.71			
17002105202	85		32.48	0.58	0.32	83.31	68.17	0.58		2.26		7.38			4.13
17002105402	87		62.23	68.66	0.05	195.65	112.04	55.28	15.72	2.65		21.06	0.57		0.04
17002105702	90		13.06	50.43	0.32	24.37	20.89	27.21				17.75	0.25		
17002106502	98		5.10	46.94		26.99	20.77	27.34			2.06	16.88	1.04		0.75

Station ID	ID	Unit	Lake	Crop land	Urban land	Conifer forest	Deciduous forest	Pasture	Alvar	Bog	Fen	Swamp	Marsh	Logging	Mining
17002106602	99			7.56		0.96	1.00	2.29				0.75			
17002106702	100		97.05	139.59	0.49	33.20	47.42	57.10				27.69	7.29		1.10
17002107002	102		1.96	43.56	9.81	11.73	14.37	23.69				9.55			0.24
17002107402	105		3.68	110.97		50.56	53.84	43.55			0.07	12.63	0.30		1.62
17002107502	106		130.98	0.82	10.47	485.81	542.35	22.72		25.85		0.59		10.82	8.65
17002107702	108		0.01	13.35		10.21	12.49	4.29				0.60			
17002109202	123	km^2	19.30	0.23	0.38	61.43	58.65	1.40		4.08	0.11	9.98			18.15
17002109502	125		45.95	3.29		196.16	278.31	5.49		2.57		16.37		2.70	1.08
17002111802	147		17.64	377.48	1.53	92.71	150.35	99.48	2.10		10.27	84.53	8.19		0.65
17002111902	148			109.69		10.87	26.18	38.33				5.05	0.02		0.21
17002112002	149		0.01	5.33		2.09	0.77	2.49				1.65			
17002113002	156		70.09	229.85	3.10	63.57	78.20	86.05			0.25	40.42	8.18		1.17
17002600202	158		6.89	141.66	0.01	120.11	121.07	55.43	1.69		0.94	67.70	0.04		0.64
17002600402	160		7.59	7.28	0.30	10.88	15.50	1.80				6.93	0.31		8.34
17002600602	162		1.65	15.02	0.35	23.69	15.91	6.23			0.86	12.44	0.23		
17002600702	163		13.13	9.43		122.66	101.84	14.69		3.34	0.29	29.86	1.57	0.78	24.35
17002600902	165		54.75	2.18		325.90	211.62	6.47		19.84	2.88	9.73	0.02	6.06	39.91
17002601002	166		21.84	6.52		212.01	132.31	9.37		9.89		17.63		0.04	20.35
17002601101	167		6.06	9.40	0.17	33.80	67.37	13.99	0.87		1.56	27.25			2.44
17002601202	168		0.57	11.94	0.77	10.71	30.82	15.04			0.07	4.94			
17002601302	169		0.47	1.32		2.72	12.03	1.51				2.84			
17002113102	173		0.03	2.61		0.92	0.97	1.33				0.14			
17002113202	174			24.24		22.78	20.21	11.95				3.98			
17002113302	175		0.72	74.90		28.15	28.79	17.62				11.76			
17002602302	176		7.01	5.89	0.68	8.19	16.05	5.76			0.01	4.75			0.23
17002113602	177		0.29	93.44		28.26	27.09	27.15			0.15	10.49	0.19		0.78
17002113702	178			18.90		4.71	4.47	4.95				0.81			0.01
17002114102	179		2.19	37.32		36.33	22.69	33.99			0.45	14.65			0.00
17002114202	180		0.69	27.95		29.46	18.46	26.56			0.08	14.85			0.32
17002114302	181		0.02	22.63		7.04	4.86	9.41				5.02			
17002114402	182		0.37	2.93	12.34	0.39	0.61	0.46				0.43			0.02
17002114002	183		0.10	72.46		25.86	28.93	22.03			0.04	5.68			0.20
17002114502	184		59.98		5.70	123.97	235.29			6.50				12.31	0.56
17000600102	186		0.01	2.84		0.03	0.99	0.41					0.66		

Station ID	ID	Unit	Lake	Crop land	Urban land	Conifer forest	Deciduous forest	Pasture	Alvar	Bog	Fen	Swamp	Marsh	Logging	Mining
17001600102	187		0.96	12.11		6.15	5.44	11.52	6.39			10.75	1.21		
17002106802	190		7.11	109.92	7.23	44.82	61.44	24.63	0.16		0.97	25.77	0.35		
17002112802	192	km^2	0.23	10.16	0.45	4.20	6.09	2.51				1.41			
17002112902	193		0.07	4.56		2.72	3.57	1.25				0.69			
17002600102	194		0.26	7.59	9.55	0.57	0.81	0.98				1.52			
17003100102	230		52.02	77.47	0.58	311.46	215.59	69.76	34.93	17.49	4.54	50.01	2.53	6.20	67.48